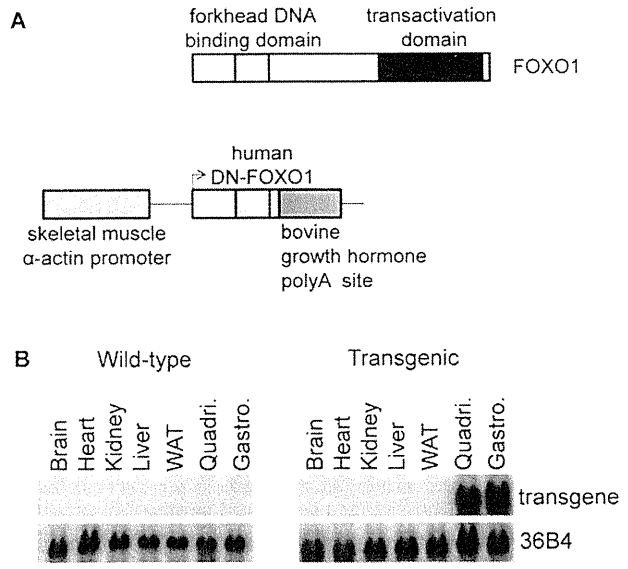

Figure 2 Creation of DN-FOXO1 transgenic mice

(**A**) The structure of FOXO1 and DN-FOXO1. DN-FOXO1 is described in the map of the 4.3-kb construct used for transgenic microinjection. The transgene was under the control of the human skeletal muscle α-actin promoter and included exon 1 and the intron of the human skeletal muscle α-actin gene as well as the bovine growth hormone polyadenylation (polyA) site. (**B**) Tissue distribution of transgene expression in DN-FOXO1 mice. RNA samples were prepared from various tissues in DN-FOXO1 and wild-type mice (male, 10 weeks of age). Northern blot analyses were conducted using the DN-FOXO1 probe and 36B4 reblotting was used as the loading control. Gastro., gastrocnemius; Quadri., quadriceps; WAT, white adipose tissue.

Transgenic mice overexpressing DN-FOXO1

Previously, we generated transgenic mice with skeletal-muscle-specific overexpression of human FOXO1 using the α-actin promoter (FOXO1 mice) [18]. Skeletal muscle in these FOXO1 mice showed an increase in *Ctsl* mRNA levels [18]. To examine the possible *in vivo* regulation of *Ctsl* by FOXO1, we also generated transgenic mice with skeletal-muscle-specific overexpression of DN-FOXO1 (Figure 2A), which suppresses FOXO1-mediated transcription. DN-FOXO1 contains the DNA-binding domain, but lacks the transcription activation domain, of FOXO1 [10,27,35]. DN-FOXO1 transgene expression was observed specifically in skeletal muscle (Figure 2B). Histologically, there was no appreciable difference in skeletal muscle between DN-FOXO1 and wild-type mice (results not shown).

Fasting-induced *Ctsl* expression is suppressed in the skeletal muscle of DN-FOXO1 mice

We used 16 DN-FOXO1 mice and 16 gender- and age-matched wild-type mice. Eight mice each were allowed to eat freely (fed) or were fasted for 24 h. *Foxo1*, *Gadd45a* and *Ctsl* expression was increased in the skeletal muscle from wild-type mice (Figure 3). In DN-FOXO1 mice, fasting-increased endogenous *Foxo1* expression was attenuated compared with wild-type mice (Figure 3A), suggesting that FOXO1 up-regulates its own gene expression. Moreover, induction of *Ctsl* as well as *Gadd45a* expression by fasting was markedly diminished in the DN-FOXO1 mice (Figures 3B and 3C). These observations indicate that FOXO1 significantly contributes to the up-regulation of *Ctsl* expression during fasting *in vivo*.

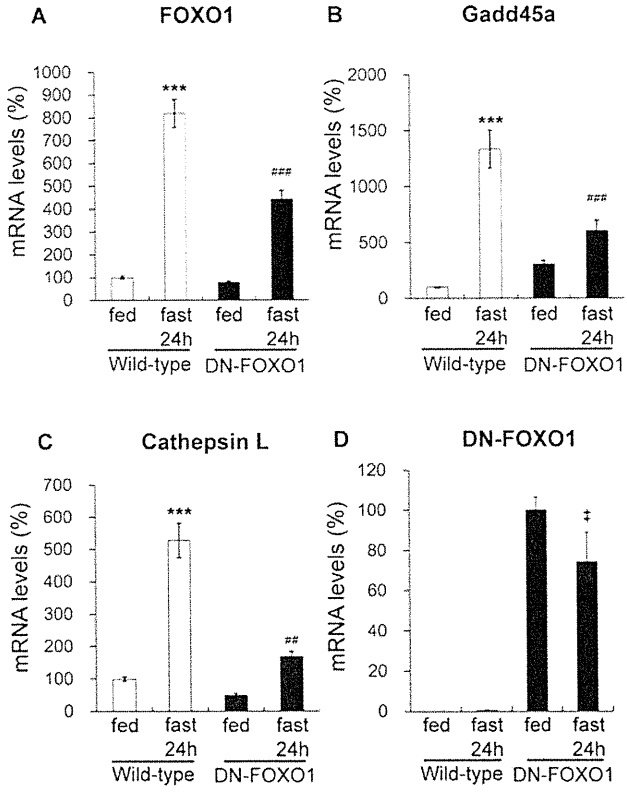

Figure 3 Gene expression in skeletal muscle of fed or fasted DN-FOXO1 mice

DN-FOXO1 mice (12 weeks of age) or age- and gender-matched wild-type mice were allowed to eat freely (fed) or subjected to a 24 h fast. The number of animals used in each group was eight. Expression of (**A**) *Foxo1* (endogenous), (**B**) *Gadd45a*, (**C**) *Ctsl* and (**D**) DN-FOXO1 (transgene) in skeletal muscle (gastrocnemius). (**A–C**) Values of wild-type mice with fed samples were set at 100. (**D**) Values of DN-FOXO1 mice with fed samples were set at 100 for DN-FOXO1 transgene. The transgene expression level was slightly decreased by fasting. Levels of mRNA were normalized to those of *36B4* mRNA. $***P < 0.001$ compared with samples of wild-type fed mice. $\#\#P < 0.01$ and $\#\#\# P < 0.001$ compared with samples of wild-type fasted mice. $\ddagger P < 0.05$ compared with samples of transgenic fed mice. Results are representative of three independent experiments with similar results.

Fasting-induced *Ctsl* expression is suppressed in the skeletal muscle of skeletal-muscle-specific *Foxo1*-knockout mice

To examine whether the induction of *Ctsl* expression in the muscles of fasting animals is dependent on FOXO1 or not, we used muscle-specific *Foxo1*-knockout mice (myogenin-cre/$Foxo1^{flox}$) [27]. Knockout and control mice were fed or were fasted for 24 h, and expression of FOXO family members (*Foxo1*, *Foxo3a* and *Foxo4*), *Ctsl* and *Gadd45a* was examined (Figure 4). In control mice, *Foxo1*, *Foxo3a*, *Ctsl* and *Gadd45a* expression was markedly up-regulated. The *Foxo1* expression in the knockout mice that were fed was much lower than that in the control mice that were fed. We did not observe marked induction of *Foxo1* expression in the fasted knockout mice relative to the fed knockout mice. In the knockout mice, the induction of *Ctsl* expression was suppressed (Figure 4C). Expression of *FOXO4* did not differ among groups (results not shown). These observations indicate that FOXO1 is important for the up-regulation of *Ctsl* expression during fasting. However, since *Ctsl* expression during fasting was not completely suppressed, there may be additional factor(s). FOXO3a may be such a factor, as its expression was up-regulated during fasting both in control and knockout mice (Figure 4D).

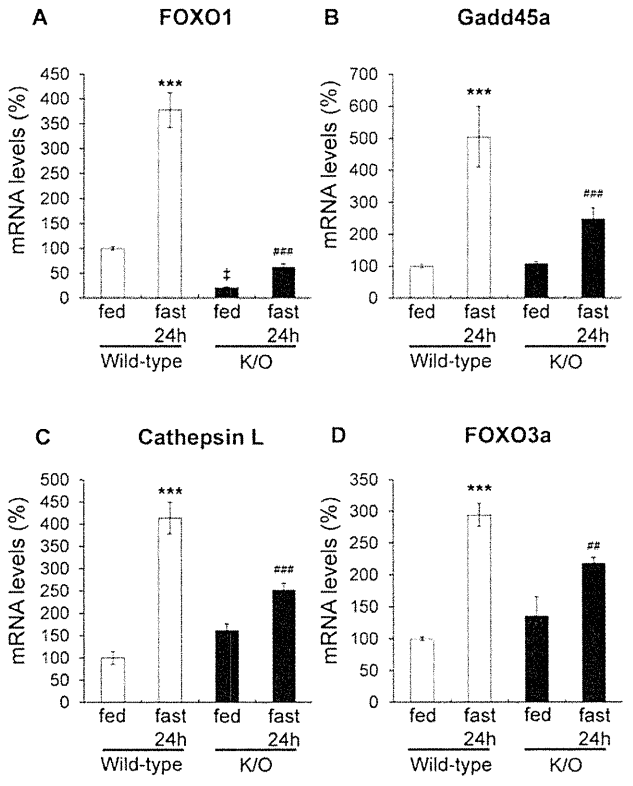

Figure 4 Gene expression in the skeletal muscle of fed or fasted muscle-specific *Foxo1*-knockout mice

Knockout (K/O) mice (4 weeks of age) or age-matched wild-type mice were allowed free access to standard chow (fed) or subjected to a 24 h fast. The number of animals used was: K/O fed, $n = 3$; K/O fast, $n = 3$; control fed, $n = 5$; control fast, $n = 4$. Expression of (**A**) *Foxo1* (endogenous), (**B**) *Gadd45a*, (**C**) *Ctsl* and (**D**) *FOXO3a* in the skeletal muscle (gastrocnemius). Values obtained in wild-type mice that were fed were set at 100. Levels of mRNA were normalized to those of *36B4* mRNA. $***P < 0.001$, relative to wild-type fed mice. $\#\# P < 0.01$ and $\#\#\# P < 0.001$ relative to wild-type fasted mice. ‡ $P < 0.05$ relative to wild-type fed mice.

Activation of FOXO1 in C2C12 myocytes promotes *Ctsl* expression

To study the effects of FOXO1 on *Ctsl* expression in muscle cells, we first employed C2C12 cells stably expressing a constitutively active form of FOXO1 [FOXO1(3A)] in-frame with a modified form of the ER ligand-binding domain that responds selectively to TAM [28]. Previous studies with these cells have shown that fusion proteins are restricted to the cytoplasmic space in the absence of ligand and then rapidly translocate to the nucleus upon treatment with TAM [28]. Each mRNA signal in Figure 5(A) is the sum of endogenous *Foxo1* mRNA and retrovirus-derived FOXO1(3A)–ER mRNA. The endogenous *Foxo1* mRNA was very low in C2C12 cells. As expected, treatment with TAM did not change FOXO1(3A)–ER mRNA levels. Treatment with TAM resulted in a marked induction of *Gadd45a* expression, confirming that it successfully promoted the transcriptional activity of our FOXO1(3A)–ER-C2C12 myotubes. As shown in Figure 5, treatment with TAM also markedly increased the mRNA abundance of *Ctsl* as well as *Gadd45a*. No changes in *Ctsl* mRNA expression were observed in FOXO1(3A)–ER cells in the absence of TAM or in control C2C12 cells stably transfected with empty vector (Mock) (Figure 5C). These results suggest that the expression of *Ctsl* is up-regulated directly by the activation of FOXO1 in muscle cells.

The mouse *Ctsl* promoter is activated by FOXO1

The above data suggest that *Ctsl* is a direct transcriptional target of FOXO1 in muscle cells. FOXO1 is known to bind the sequence GTAAACAA or DBE [32]. We therefore examined using a transient transfection-reporter assay whether the mouse *Ctsl* and human *CTSL1* promoters are activated by FOXO1. The mouse *Ctsl* promoter has been cloned previously [29]. We sequenced the 4-kb mouse *Ctsl* promoter and found a single consensus FOXO1-binding site (GTAAACAA) (−3528 to −3535, numbering the first nucleotide of exon 1 as +1). Plasmid constructs linking the mouse *Ctsl* promoter including the putative FOXO1-binding site to the luciferase reporter gene were analysed. FOXO1 increased the mouse *Ctsl* promoter (−4000 to +10)-driven reporter activity (Figure 6A). Furthermore, mutation in the consensus FOXO1-binding site abolished the FOXO1-induced luciferase activity (Figure 6A). Consistent with *in vivo* transgenic mice data (Figure 3), in the *in vitro* transfection reporter assay, DN-FOXO1 dose-dependently suppressed the FOXO1(3A)-induced transcriptional activity of the mouse *Ctsl* promoter (Figure 6B). These observations suggest that FOXO1 up-regulates the mouse *Ctsl* expression via the DBE sequence in its promoter.

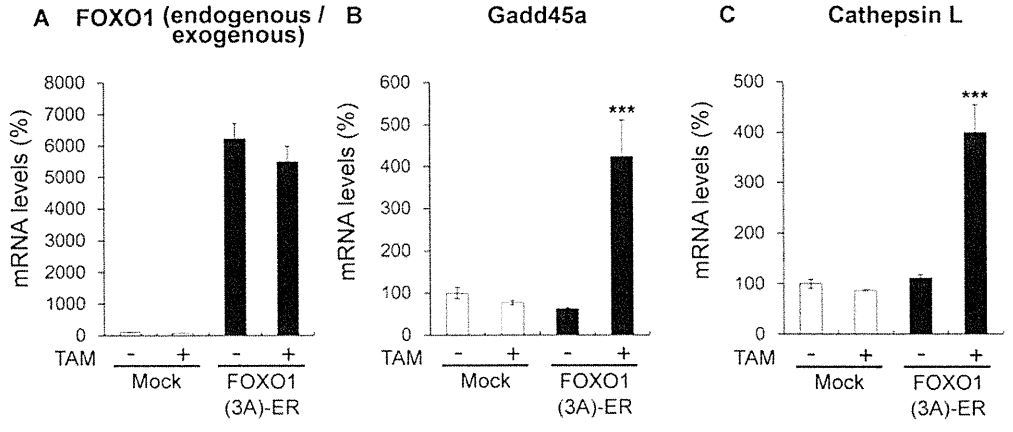

Figure 5 *Ctsl* expression by FOXO1 in C2C12 muscle cells

The abundance of mRNA transcripts for (**A**) *Foxo1*, (**B**) *Gadd45a* and (**C**) *Ctsl* in control (mock, open bars) and FOXO1(3A)–ER C2C12 cells (closed bars) treated with (+) or without (−) TAM for 24 h was analysed by quantitative real-time PCR. Levels of mRNA were normalized to those of *36B4* mRNA. $***P < 0.001$ compared with samples without TAM.

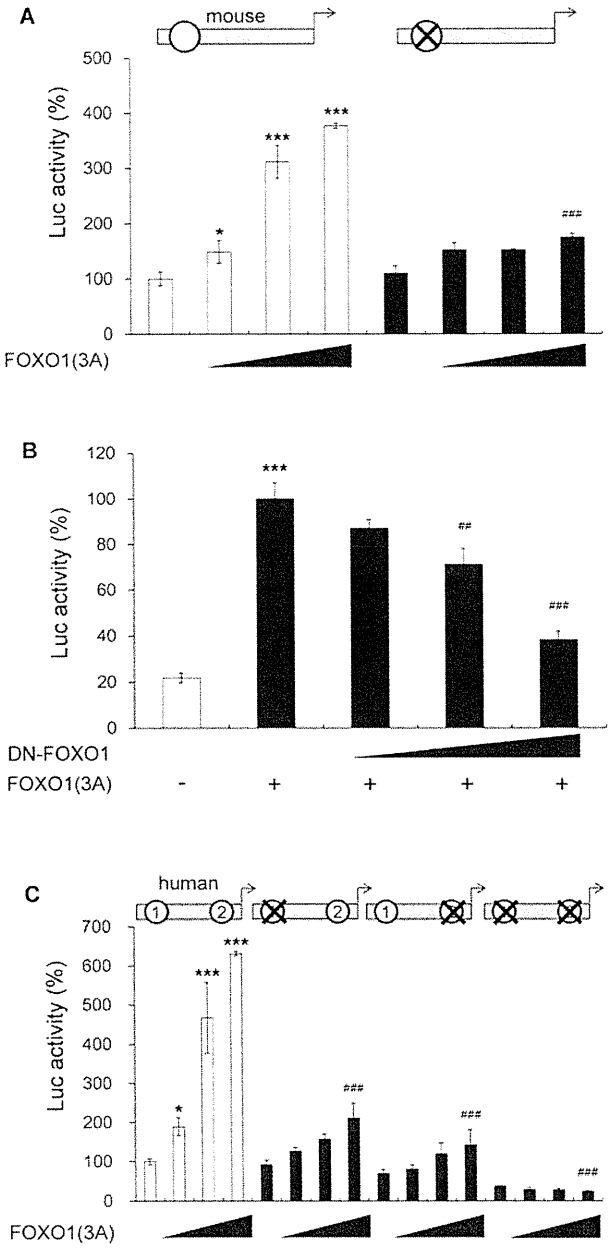

Figure 6 Transient transfection-reporter assay of the effect of FOXO1 on *Ctsl* promoters

The effect of increasing the amount of FOXO1 was examined by co-transfection with the reporter plasmids in HEK-293 cells. (**A**) The mouse *Ctsl* promoter (−4 kb) with mutations in putative FOXO1-binding sites. (**C**) The human *CTSL1* promoter (−1.6 kb) with mutations in the putative FOXO1-binding site. Activation of the luciferase reporter gene was measured in relative light units and was normalized to the dual-luciferase activity. Mean values from triplicate experiments are shown as the fold-induction, where the activity in the absence of FOXO1 is the reference value (set at 100). Schematic representations of *Ctsl* and *CTSL1* promoter constructs are shown above the histograms. Circles denote the putative FOXO1-binding sites and crosses denote mutations in the FOXO1-binding sites. Number in the circles: 1 is DBE1 (−1400 to −1407) and 2 is DBE2 (−145 to −152, numbering the first nucleotide of exon 1 as +1). $^{*}P < 0.05$ and $^{***}P < 0.001$ compared with the value of wild-type promoter in the absence of FOXO1(3A). $\#\#\#P < 0.001$ compared with the values of wild-type promoter with the largest amount of FOXO1(3A). (**B**) Transient transfection assay of the DN-FOXO1 construct used to suppress FOXO1-mediated transactivation *in vitro*. The effect of DN-FOXO1 was examined by co-transfection of the reporter plasmid containing the mouse *Ctsl* promoter with or without pCAG-FOXO1(3A). An increasing amount of DN-FOXO1 suppressed FOXO1(3A)-induced *Ctsl* promoter activity. Activation of the luciferase reporter gene was measured in relative light units and normalized to the dual-luciferase activity. Mean values from triplicate experiments are shown as the fold-induction, where the activity in the absence of DN-FOXO1 and in the presence of FOXO1(3A) is the reference value (set at 100). $^{***}P < 0.001$ compared with the value in the absence of DN-FOXO1 and FOXO1(3A). $\#\#P < 0.01$; and $\#\#\#P < 0.001$ compared with the value in the absence of DN-FOXO1 and in the presence of FOXO1(3A).

The human *CTSL1* promoter is bound and activated by FOXO1

In the human *CTSL1* promoter [30,31], we also found two potential FOXO-binding sites; there are two perfect DBEs (−145 to −152 and −1400 to −1407, numbering the first nucleotide of exon 1 as +1). FOXO1 increased the human *CTSL1* promoter (−1600 to +10)-driven reporter activity in a transfection assay (Figure 6C). In addition, mutations in the consensus DBEs abolished the FOXO1-induced luciferase activity. Thus the results of the luciferase assay with the human *CTSL1* promoter were similar to those with the mouse *Ctsl* promoters.

We also examined the binding of FOXO1 to the DBEs in the human *CTSL1* promoter with a gel mobility-shift assay. FOXO1 that was synthesized *in vitro* clearly bound to oligonucleotides containing the putative FOXO1-binding sites of the human *CTSL1* promoter, and did not bind to oligonucleotides with mutations in the consensus DBEs (Figure 7A). Moreover, we performed a ChIP analysis using C2C12 cells expressing FOXO1(3A)–ER (as used in Figure 5), and found that FOXO1 was recruited to the mouse *Ctsl* promoter containing the DBE (Figure 7B). These observations, taken together, suggest that FOXO1 up-regulates the mouse *Ctsl* and human *CTSL1* expression via the DBE sequences of their promoters; *CTSL1* is a direct target of FOXO1 in the skeletal muscle.

DISCUSSION

FOXO1 signalling is important in linking nutritional and hormonal cascades to the regulation of skeletal muscle atrophy. As a transcriptional factor and/or cofactor, FOXO1 regulates many genes in a variety of biological processes. Identification and molecular analysis of FOXO1 target genes should help facilitate a better understanding of skeletal muscle metabolism. In the present study, we showed that FOXO1 directly activates *Ctsl* expression.

In the present study, we first conducted *in vivo* experiments focusing on FOXO1 regulation of *Ctsl* expression in skeletal muscle in the context of physiological nutritional change. During fasting and refeeding of C57BL6 mice, *Ctsl* was regulated in parallel with FOXO1 in skeletal muscle (Figure 1). Fasting-induced *Ctsl* expression was attenuated in DN-FOXO1 mice (Figure 3) and in skeletal-muscle-specific *Foxo1*-knockout mice (Figure 4) relative to respective wild-type controls. In this regard, we observed previously that *Ctsl* expression is markedly increased in skeletal muscle of FOXO1 mice [18]. Taken together, our results suggest that FOXO1 activates *Ctsl* expression *in vivo*. The increase in *Ctsl* mRNA is delayed compared with that of *Foxo1* (Figure 1). This could be explained as follows: (i) *Ctsl* mRNA may have a long half life, or (ii) *Ctsl* is activated by different transcription factors as well as FOXO1 during fasting. Indeed, it has been reported that addition of glucocorticoid, whose blood level is increased during fasting, has been reported to increase the level of *Ctsl* mRNA [20]. Cathepsin L is considered to play a major role in the terminal degradation of proteins delivered to lysosomes by endocytosis or autophagy [24,36]. A previous study shows that pharmacological inhibition in rats of both cathepsin L and calpain, an intracellular Ca^{2+}-dependent

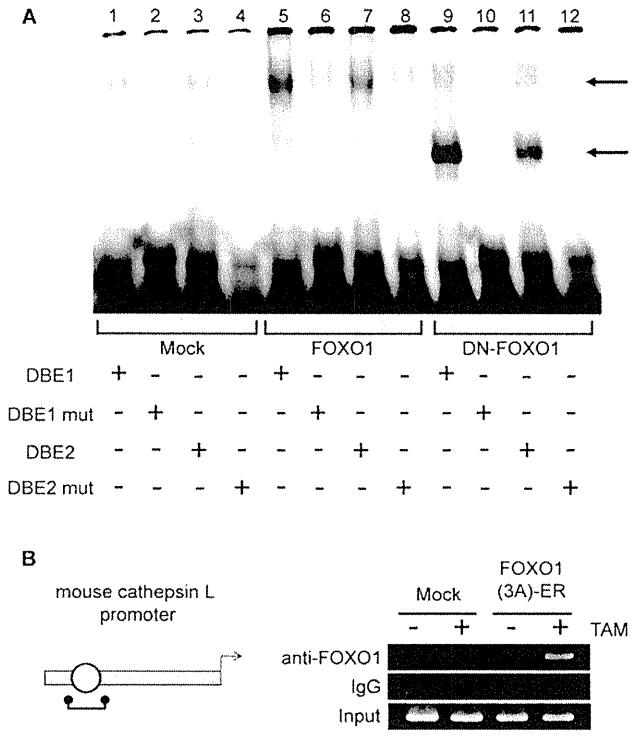

Figure 7 Recruitment of FOXO1 to the putative FOXO1-binding sites of the *Ctsl* promoter

(**A**) Gel mobility-shift assay. Synthetic double-stranded oligonucleotides containing putative FOXO1-binding sites of the human *CTSL1* promoter were used. *In vitro* synthesized FOXO1 protein was incubated with ^{32}P-labelled double-stranded oligonucleotides (DBE1, −1400 to −1407; DBE2, −145 to −152, numbering the first nucleotide of exon 1 as + 1; or DBE1 mut and DBE2 mut, oligonucleotides with mutation in the consensus sequence) for 30 min on ice. The protein–DNA complexes were resolved on an 8% non-denaturing gel. FOXO1 and DN-FOXO1 were able to bind labelled *CTSL1* oligonucleotides (FOXO1, lanes 5 and 7; DN-FOXO1, lanes 9 and 11), but not mutated oligonucleotides (FOXO1, lanes 6 and 8; DN-FOXO1, lanes 10 and 12). The arrows indicate the specific protein–DNA complex. (**B**) ChIP assay. Primers specific to the region of the mouse *Ctsl* promoter containing the DBE were used for PCR analysis. FOXO1(3A)–ER was recruited to the *Ctsl* promoter in the presence of TAM. No signals were detected using control IgG. Primers corresponding to the region of non-DBE did not give any signals (not shown).

protease, prevents sepsis-induced bulk protein degradation [37] and suggests a role for cathepsin L in the degradation of various skeletal muscle proteins. It is therefore conceivable that FOXO1-induced transcriptional activation of *Ctsl* plays a role in fasting-induced autophagy and proteolysis. During fasting, a large number of genes show a change in their expression; some are changed directly as a physiological response, and others may be changed indirectly as secondary events. Nevertheless, *Ctsl* expression is likely to be regulated by FOXO1.

Using C2C12 myoblasts, we also showed that FOXO1 induces endogenous *Ctsl* expression *in vitro* (Figure 5). Moreover, we showed that FOXO1 can bind to and activate the *Ctsl* promoter (Figures 6 and 7). The promoter of *Ctsl* has been sequenced and analysed in humans, mice and rats. Transcription factors such as the specificity proteins Sp1/Sp3 have been reported to increase the basal activities of the promoter [31,38,39]. In the present study, we have provided the first evidence for transcriptional activation of the *Ctsl* promoter by an inducible transcription factor, FOXO1, thereby suggesting that *Ctsl* is a direct target gene of FOXO1. During fasting, among members of the cathepsin family, only *Ctsl* expression is markedly increased in skeletal muscle [21]. Indeed, there are no consensus DBEs in the putative promoter of other cathepsins (−1.5 kb from the transcription start sites of cathepsins B, C, D, E, G, H, J, K S and Z in humans and mice; Y. Yamazaki and Y. Kamei, unpublished work), indicating that FOXO1 specifically activates *Ctsl* during fasting. Therefore cathepsin L probably plays a role in fasting-induced adaptive responses including skeletal muscle atrophy.

FOXO1 has been shown to activate the expression of *Gadd45a*, *Pepck* and *G6Pase* via direct binding to DBE *in vitro* [19,40]. On the other hand, adenoviral introduction of DN-FOXO1 can suppress the gene expression of *Pepck* and *G6Pase* in the liver *in vivo* [10]. Previous studies suggest that FOXO1 can regulate gene expression in at least two different ways: (i) FOXO1 directly binds to and transactivates the promoter of its target genes [32], or (ii) FOXO1 interacts with other transcription factors via protein–protein interactions, without DNA binding, thereby regulating the expression of target genes [27,41]. Because FOXO1 interacts with nuclear receptors via its C-terminus [41], DN-FOXO1 can suppress the action of FOXO1 as a transcription factor without affecting its action as a transcriptional cofactor. Therefore FOXO1 appears to regulate *Ctsl* expression via a transcriptional mechanism.

We reported previously that FOXO1 mice have decreased skeletal muscle mass [18]. In the present study, there was no appreciable histological difference in skeletal muscle between DN-FOXO1 and wild-type mice. We also observed no marked difference in body weight and skeletal muscle mass between DN-FOXO1 and wild-type mice (results not shown). This may be because DN-FOXO1 does not suppress all the FOXO1 actions in a dominant-negative fashion, as described in the above. A detailed phenotypic analysis of DN-FOXO1 mice is ongoing in our laboratory.

In conclusion, the present study provides *in vivo* and *in vitro* evidence that *Ctsl* is a direct target of FOXO1 in skeletal muscle. The results provide important clues towards understanding the molecular mechanism underlying FOXO1-mediated transcriptional regulation of gene expression in skeletal muscle. Further studies will better clarify the physiological and pathophysiological implication of FOXO1-induced *Ctsl* expression in skeletal muscle.

AUTHOR CONTRIBUTION

Yasutomi Kamei, Tadahiro Kitamura, Takayoshi Suganami, Osamu Ezaki and Yoshihiro Ogawa led the design and overall implementation of the trial. Yasutomi Kamei wrote the initial draft of the paper in consultation with Yukio Hirata, Bruce Troen and Yoshihiro Ogawa. Yoshihiro Yamazaki, Satoshi Sugita, Fumiko Akaike, Sayaka Kanai, Shinji Miura and Ichizo Nishino were responsible for laboratory analyses. All authors contributed to interpretation of data and have seen and approved the final manuscript.

ACKNOWLEDGEMENTS

We thank Ms Chihiro Osawa for technical assistance of *Foxo1*-knockout mice analysis. We thank Dr Terry G. Unterman for providing the FOXO1(3A)–ER plasmid. S. Sugita is a Research Fellow of the Japan Society for the Promotion of Science.

FUNDING

This work was supported in part by a Grant-in-Aid for scientific research KAKENHI from the Japanese Ministry of Education, Culture, Sports, Science and Technology (MEXT, Tokyo, Japan), from the Japanese Ministry of Health, Labour and Welfare, and research grants from Astellas Foundation for Research on Metabolic Disorders, Ono Medical Research Foundation, Takeda Science Foundation, and Novo Nordisk Pharma Ltd Insulin Research 2009.

REFERENCES

1 Berchtold, M. W., Brinkmeier, H. and Muntener, M. (2000) Calcium ion in skeletal muscle: its crucial role for muscle function, plasticity, and disease. Physiol. Rev. **80**, 1215–1265
2 Glass, D. J. (2003) Molecular mechanisms modulating muscle mass. Trends Mol. Med. **9**, 344–350
3 Salway, J. G. (1999) Metabolism at a Glance. 2nd edn Blackwell Science, Oxford
4 Anderson, M. J., Viars, C. S., Czekay, S., Cavenee, W. K. and Arden, K. C. (1998) Cloning and characterization of three human forkhead genes that comprise an FKHR-like gene subfamily. Genomics **47**, 187–199
5 Kaestner, K. H., Knochel, W. and Martinez, D. E. (2000) Unified nomenclature for the winged helix/forkhead transcription factors. Genes Dev. **14**, 142–146
6 Accili, D. and Arden, K. C. (2004) FoxOs at the crossroads of cellular metabolism, differentiation, and transformation. Cell **117**, 421–426
7 Barthel, A., Schmoll, D. and Unterman, T. G. (2005) FoxO proteins in insulin action and metabolism. Trends Endocrinol. Metab. **16**, 183–189
8 Nakae, J., Oki, M. and Cao, Y. (2008) The FoxO transcription factors and metabolic regulation. FEBS Lett. **582**, 54–67
9 Daitoku, H. and Fukamizu, A. (2007) FOXO transcription factors in the regulatory networks of longevity. J. Biochem. **141**, 769–774
10 Altomonte, J., Richter, A., Harbaran, S., Suriawinata, J., Nakae, J., Thung, S. N., Meseck, M., Accili, D. and Dong, H. (2003) Inhibition of Foxo1 function is associated with improved fasting glycemia in diabetic mice. Am. J. Physiol. Endocrinol. Metab. **285**, E718–E728
11 Kamei, Y., Mizukami, J., Miura, S., Suzuki, M., Takahashi, N., Kawada, T., Taniguchi, T. and Ezaki, O. (2003) A forkhead transcription factor FKHR up-regulates lipoprotein lipase expression in skeletal muscle. FEBS Lett. **536**, 232–236
12 Furuyama, T., Kitayama, K., Yamashita, H. and Mori, N. (2003) Forkhead transcription factor FOXO1 (FKHR)-dependent induction of *PDK4* gene expression in skeletal muscle during energy deprivation. Biochem. J. **375**, 365–371
13 Kamei, Y., Miura, S., Suganami, T., Akaike, F., Kanai, S., Sugita, S., Katsumata, A., Aburatani, H., Unterman, T. G., Ezaki, O. and Ogawa, Y. (2008) Regulation of *SREBP1c* gene expression in skeletal muscle: role of retinoid X receptor/liver X receptor and forkhead-O1 transcription factor. Endocrinology **149**, 2293–2305
14 Sandri, M., Sandri, C., Gilbert, A., Skurk, C., Calabria, E., Picard, A., Walsh, K., Schiaffino, S., Lecker, S. H. and Goldberg, A. L. (2004) Foxo transcription factors induce the atrophy-related ubiquitin ligase atrogin-1 and cause skeletal muscle atrophy. Cell **117**, 399–412
15 Stitt, T. N., Drujan, D., Clarke, B. A., Panaro, F., Timofeyva, Y., Kline, W. O., Gonzalez, M., Yancopoulos, G. D. and Glass, D. J. (2004) The IGF-1/PI3K/Akt pathway prevents expression of muscle atrophy-induced ubiquitin ligases by inhibiting FOXO transcription factors. Mol. Cell **14**, 395–403
16 Zhao, J., Brault, J. J., Schild, A., Cao, P., Sandri, M., Schiaffino, S., Lecker, S. H. and Goldberg, A. L. (2007) FoxO3 coordinately activates protein degradation by the autophagic/lysosomal and proteasomal pathways in atrophying muscle cells. Cell Metab. **6**, 472–483
17 Mammucari, C., Milan, G., Romanello, V., Masiero, E., Rudolf, R., Del Piccolo, P., Burden, S. J., Di Lisi, R., Sandri, C., Zhao, J. et al. (2007) FoxO3 controls autophagy in skeletal muscle *in vivo*. Cell Metab. **6**, 458–471
18 Kamei, Y., Miura, S., Suzuki, M., Kai, Y., Mizukami, J., Taniguchi, T., Mochida, K., Hata, T., Matsuda, J., Aburatani, H. et al. (2004) Skeletal muscle FOXO1 (FKHR) transgenic mice have less skeletal muscle mass, down-regulated Type I (slow twitch/red muscle) fiber genes, and impaired glycemic control. J. Biol. Chem. **279**, 41114–41123
19 Furukawa-Hibi, Y., Yoshida-Araki, K., Ohta, T., Ikeda, K. and Motoyama, N. (2002) FOXO forkhead transcription factors induce G_2–M checkpoint in response to oxidative stress. J. Biol. Chem. **277**, 26729–26732
20 Deval, C., Mordier, S., Obled, C., Bechet, D., Combaret, L., Attaix, D. and Ferrara, M. (2001) Identification of cathepsin L as a differentially expressed message associated with skeletal muscle wasting. Biochem. J. **360**, 143–150
21 Lecker, S. H., Jagoe, R. T., Gilbert, A., Gomes, M., Baracos, V., Bailey, J., Price, S. R., Mitch, W. E. and Goldberg, A. L. (2004) Multiple types of skeletal muscle atrophy involve a common program of changes in gene expression. FASEB J. **18**, 39–51
22 Sacheck, J. M., Hyatt, J. P., Raffaello, A., Jagoe, R. T., Roy, R. R., Edgerton, V. R., Lecker, S. H. and Goldberg, A. L. (2007) Rapid disuse and denervation atrophy involve transcriptional changes similar to those of muscle wasting during systemic diseases. FASEB J. **21**, 140–155
23 Furuno, K., Goodman, M. N. and Goldberg, A. L. (1990) Role of different proteolytic systems in the degradation of muscle proteins during denervation atrophy. J. Biol. Chem. **265**, 8550–8557
24 Bechet, D., Tassa, A., Taillandier, D., Combaret, L. and Attaix, D. (2005) Lysosomal proteolysis in skeletal muscle. Int. J. Biochem. Cell Biol. **37**, 2098–2114
25 Brennan, K. J. and Hardeman, E. C. (1993) Quantitative analysis of the human α-skeletal actin gene in transgenic mice. J. Biol. Chem. **268**, 719–725
26 Nakae, J., Barr, V. and Accili, D. (2000) Differential regulation of gene expression by insulin and IGF-1 receptors correlates with phosphorylation of a single amino acid residue in the forkhead transcription factor FKHR. EMBO J. **19**, 989–996
27 Kitamura, T., Kitamura, Y. I., Funahashi, Y., Shawber, C. J., Castrillon, D. H., Kollipara, R., DePinho, R. A., Kitajewski, J. and Accili, D. (2007) A Foxo/Notch pathway controls myogenic differentiation and fiber type specification. J. Clin. Invest. **117**, 2477–2485
28 Bastie, C. C., Nahle, Z., McLoughlin, T., Esser, K., Zhang, W., Unterman, T. and Abumrad, N. A. (2005) FoxO1 stimulates fatty acid uptake and oxidation in muscle cells through CD36-dependent and -independent mechanisms. J. Biol. Chem. **280**, 14222–14229
29 Troen, B. R., Chauhan, S. S., Ray, D. and Gottesman, M. M. (1991) Downstream sequences mediate induction of the mouse cathepsin L promoter by phorbol esters. Cell Growth Differ. **2**, 23–31
30 Bakhshi, R., Goel, A., Seth, P., Chhikara, P. and Chauhan, S. S. (2001) Cloning and characterization of human cathepsin L promoter. Gene **275**, 93–101
31 Jean, D., Guillaume, N. and Frade, R. (2002) Characterization of human cathepsin L promoter and identification of binding sites for NF-Y, Sp1 and Sp3 that are essential for its activity. Biochem. J. **361**, 173–184
32 Furuyama, T., Nakazawa, T., Nakano, I. and Mori, N. (2000) Identification of the differential distribution patterns of mRNAs and consensus binding sequences for mouse DAF-16 homologues. Biochem. J. **349**, 629–634
33 Kamei, Y., Xu, L., Heinzel, T., Torchia, J., Kurokawa, R., Gloss, B., Lin, S. C., Heyman, R. A., Rose, D. W., Glass, C. K. and Rosenfeld, M. G. (1996) A CBP integrator complex mediates transcriptional activation and AP-1 inhibition by nuclear receptors. Cell **85**, 403–414
34 Suganami, T., Yuan, X., Shimoda, Y., Uchio-Yamada, K., Nakagawa, N., Shirakawa, I., Usami, T., Tsukahara, T., Nakayama, K., Miyamoto, Y. et al. (2009) Activating transcription factor 3 constitutes a negative feedback mechanism that attenuates saturated fatty acid/Toll-like receptor 4 signaling and macrophage activation in obese adipose tissue. Circ. Res. **105**, 25–32
35 Hribal, M. L., Nakae, J., Kitamura, T., Shutter, J. R. and Accili, D. (2003) Regulation of insulin-like growth factor-dependent myoblast differentiation by Foxo forkhead transcription factors. J. Cell Biol. **162**, 535–541
36 Barrett, A. J. and Kirschke, H. (1981) Cathepsin B, cathepsin H, and cathepsin L. Methods Enzymol. **80**, 535–561
37 Fareed, M. U., Evenson, A. R., Wei, W., Menconi, M., Poylin, V., Petkova, V., Pignol, B. and Hasselgren, P. O. (2006) Treatment of rats with calpain inhibitors prevents sepsis-induced muscle proteolysis independent of atrogin-1/MAFbx and MuRF1 expression. Am. J. Physiol. Regul. Integr. Comp. Physiol. **290**, R1589–R1597
38 Charron, M., DeCerbo, J. N. and Wright, W. W. (2003) A GC-box within the proximal promoter region of the rat cathepsin L gene activates transcription in Sertoli cells of sexually mature rats. Biol. Reprod. **68**, 1649–1656
39 Sriraman, V. and Richards, J. S. (2004) Cathepsin L gene expression and promoter activation in rodent granulose cells. Endocrinology **145**, 582–591
40 Barthel, A., Schmoll, D., Kruger, K. D., Bahrenberg, G., Walther, R., Roth, R. A. and Joost, H. G. (2001) Differential regulation of endogenous glucose-6-phosphatase and phosphoenolpyruvate carboxykinase gene expression by the forkhead transcription factor FKHR in H4IIE-hepatoma cells. Biochem. Biophys. Res. Commun. **285**, 897–902
41 van der Vos, K. E. and Coffer, P. J. (2008) FOXO-binding partners: it takes two to tango. Oncogene **27**, 2289–2299

Received 28 August 2009/19 January 2009; accepted 20 January 2010
Published as BJ Immediate Publication 20 January 2010, doi:10.1042/BJ20091346

Biochem. J. (2010) **427**, 171–178 (Printed in Great Britain) doi:10.1042/BJ20091346

online data

SUPPLEMENTARY ONLINE DATA

The cathepsin L gene is a direct target of FOXO1 in skeletal muscle

Yoshihiro YAMAZAKI*†‡, Yasutomi KAMEI*[1], Satoshi SUGITA*, Fumiko AKAIKE*, Sayaka KANAI*, Shinji MIURA§, Yukio HIRATA‡, Bruce R. TROEN‖, Tadahiro KITAMURA¶, Ichizo NISHINO**, Takayoshi SUGANAMI*, Osamu EZAKI§ and Yoshihiro OGAWA*†

*Department of Molecular Medicine and Metabolism, Tokyo Medical and Dental University, 1-5-45 Yushima, Bunkyo-ku, Tokyo 113-8510, Japan, †Global Center of Excellence Program, International Research Center for Molecular Science in Tooth and Bone Diseases, Medical Research Institute, Tokyo Medical and Dental University, 1-5-45 Yushima, Bunkyo-ku, Tokyo 113-8510, Japan, ‡Department of Clinical and Molecular Endocrinology, Tokyo Medical and Dental University, 1-5-45 Yushima, Bunkyo-ku, Tokyo 113-8510, Japan, §Nutritional Science Program, National Institute of Health and Nutrition, Tokyo 162-8636, Japan, ‖Geriatrics Research, Education and Clinical Center and Research Service, Miami Veterans Affairs Healthcare System, and Geriatrics Institute, Department of Medicine, Miller School of Medicine, University of Miami, Miami FL 33125, U.S.A., ¶Metabolic Signal Research Center, Institute for Molecular and Cellular Regulation, Gunma University, Maebashi, Gunma 371-8512, Japan, and **Department of Neuromuscular Research, National Institute of Neuroscience, National Center of Neurology and Psychiatry, Tokyo 187-8502, Japan

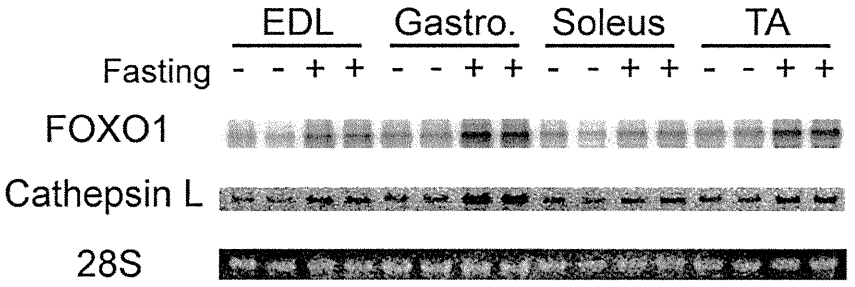

Figure S1 ***Foxo1*** **and** ***Ctsl*** **expression in various regions of skeletal muscle of fasted mice**

Mice (C57BL6, male, 8 weeks of age) were either allowed free access to standard chow (fed) or subjected to a 24 h fast. Mice were killed, and relative mRNA levels of *Foxo1* and *Ctsl* were examined by Northern blot analysis. RNA samples were prepared from indicated skeletal muscles. The 28S staining used as the loading control gave similar abundance. EDL, extensor digitorum longus; Gastro., gastrocnemius; TA, tibialis anterior.

Received 28 August 2009/19 January 2009; accepted 20 January 2010
Published as BJ Immediate Publication 20 January 2010, doi:10.1042/BJ20091346

[1] To whom correspondence should be addressed (email kamei.mmm@mri.tmd.ac.jp).

サルコメア配列異常を主病変とする筋ジストロフィーの

病因・病態の解明と治療法の開発

Acta Neuropathol (2010) 119:481–486
DOI 10.1007/s00401-010-0660-7

ORIGINAL PAPER

Congenital myotonic dystrophy can show congenital fiber type disproportion pathology

Kayo Tominaga · Yukiko K. Hayashi · Kanako Goto · Narihiro Minami · Satoru Noguchi · Ikuya Nonaka · Tetsuro Miki · Ichizo Nishino

Received: 19 November 2009 / Revised: 15 February 2010 / Accepted: 15 February 2010 / Published online: 24 February 2010

Abstract Congenital myotonic dystrophy (CDM) is associated with markedly expanded CTG repeats in *DMPK*. The presence of numerous immature fibers with peripheral halo is a characteristic feature of CDM muscles together with hypotrophy of type 1 fibers. Smaller type 1 fibers with no structural abnormality are a definitive criterion of congenital fiber type disproportion (CFTD). Nonetheless, we recently came across a patient who was genetically confirmed as CDM, but had been earlier diagnosed as CFTD when he was an infant. In this study, we performed clinical, pathological, and genetic analyses in infantile patients pathologically diagnosed as CFTD to evaluate CDM patients indistinguishable from CFTD. We examined CTG repeat expansion in *DMPK* in 28 infantile patients pathologically diagnosed as CFTD. Mutation screening of *ACTA1* and *TPM3* was performed, and we compared clinical and pathological findings of 20 CDM patients with those of the other cohorts. We identified four (14%) patients with CTG expansion in *DMPK*. *ACTA1* mutation was identified in four (14%), and *TPM3* mutation was found in two (7%) patients. Fiber size disproportion was more prominent in patients with *ACTA1* or *TPM3* mutations as compared to CFTD patients with CTG expansion. A further three patients among 20 CDM patients showed pathological findings similar to CFTD. From our results, CDM should be excluded in CFTD patients.

Keywords Congenital myotonic dystrophy (CDM) · Congenital fiber type disproportion (CFTD) · *DMPK* · CTG expansion · *ACTA1* · *TPM3*

Introduction

Congenital myotonic dystrophy (CDM; OMIM 160900) is caused by marked expansion of trinucleotide (CTG) repeat in the 3′ untranslated region of the dystrophia myotonica protein kinase gene (*DMPK*; OMIM 605377) on chromosome 19q [1, 5, 9]. The CTG repeat in normal individuals varies from 5 to 35, whereas it expands to more than 1,000 repeats in CDM [7]. Typically, the mothers of CDM patients show clinical features of myotonic dystrophy which makes the diagnosis of CDM easier. Clinically, CDM patients show hypotrophy at birth, tented upper lip, facial muscle weakness, and neonatal respiratory insufficiency. Mental retardation becomes evident in later life. On muscle pathology, the presence of numerous immature fibers with peripheral halo is a characteristic feature together with increased number of fibers with centrally placed nuclei and hypotrophy of type 1 fibers, mimicking myotubular myopathy [6].

Smaller sized type 1 fibers as compared to type 2 fibers are a characteristic pathological feature of congenital fiber type disproportion (CFTD; OMIM 255310). CFTD is a

Electronic supplementary material The online version of this article (doi:10.1007/s00401-010-0660-7) contains supplementary material, which is available to authorized users.

K. Tominaga · Y. K. Hayashi · K. Goto · N. Minami · S. Noguchi · I. Nonaka · I. Nishino (✉)
Department of Neuromuscular Research, National Institute of Neuroscience, National Center of Neurology and Psychiatry, 4-1-1 Ogawa-higashi, Kodaira, Tokyo 187-8502, Japan
e-mail: nishino@ncnp.go.jp

T. Miki
Proteo-Medicine Research Center, Ehime University, Toon, Ehime 791-0295, Japan

K. Tominaga · T. Miki
Department of Geriatric Medicine, Ehime University Graduate School of Medicine, Toon, Ehime 791-0295, Japan

congenital myopathy defined by type 1 fiber hypotrophy of 12% or more than type 2 fibers, and with the absence of structural abnormalities within myofibers [2]. Type 1 fiber predominance is also commonly seen. Clinically, CFTD patients show hypotonia, facial muscle weakness, and severe respiratory insufficiency at birth. Long face, high-arched palate, and joint contractures are often seen. CFTD is a genetically heterogeneous disorder and mutations in the genes for tropomyosin 3 (*TPM3*; OMIM 191030), α-skeletal muscle actin 1 (*ACTA1*; OMIM 102610), and selenoprotein N1 (*SEPN1*; OMIM 606210) have been identified [3, 4, 8]. Reportedly *TPM3* mutations are the most common ones and observed approximately in 20–25% of the CFTD patients [4]. *ACTA1* mutations were identified in 6% of CFTD [8], and only one family was reported having an *SEPN1* mutation [3].

Although the muscle pathology features of CDM seem to be well defined, our experience with one CDM patient who was previously diagnosed as CFTD made us hypothesize that CDM may have features other than the presently defined ones, both in terms of muscle pathology and clinical characteristics. In this study, we looked for CDM patients among patients who presented with CFTD. We also performed clinical and pathological analysis to find out whether patients with CDM can be distinguished from CFTD.

Materials and methods

Patients

All clinical materials used in this study were obtained for diagnostic purposes and with informed consent. This work was approved by the Ethical Committee of National Center of Neurology and Psychiatry (NCNP). In this study, we chose muscle specimens from patients younger than 1 year of age. From the muscle repository of NCNP, there were 28 unrelated patients who were pathologically diagnosed as CFTD. Twenty CDM patients, who had symptomatic family members and whose diagnosis was genetically confirmed, were also used for comparison.

Histochemistry

Biopsied skeletal muscles were frozen with isopentane cooled in liquid nitrogen. Serial frozen sections of 10 μm thickness were stained with hematoxylin and eosin (H & E), modified Gomori-trichrome (mGT), NADH-tetrazolium reductase (NADH-TR), and ATPases (pH 10.6, pH 4.6 and pH 4.3). For each muscle specimen, the mean fiber diameter was determined by obtaining the shortest anteroposterior diameter of 100 each of type 1 and type 2 (A + B) fibers using ATPase stains. The myofiber diameter was used to calculate the fiber size disproportion (FSD). FSD was computed as: difference of type 2 fiber diameter (mean) and type 1 fiber diameter (mean) divided by type 2 fiber diameter (mean) × 100%.

Genetic analyses

Genomic DNA was extracted from peripheral lymphocytes or frozen muscle specimens using standard protocol. To examine CTG repeat expansion in *DMPK*, triplet repeat primed PCR was performed as described previously [12]. The presence of the expanded CTG repeats was examined by Gene Mapper using ABI PRISM 310 automated sequencer (Applied Biosystems Japan Co., Ltd, Japan). To know the approximate number of triplet repeats, we performed Southern blotting analysis using PCR-amplified CTG repeats because of the limited amounts of muscle specimens [10]. The primer sequences used in this study are F: 5′-CGAACGGGGCTCGAAGGGTCCTTGTAGC CG-3′, and R: 5′-TCTTTCTTTACCAGACACTAGGG-3′.

The PCR products were electrophoresed with 1% of Seakem HGT agarose gel (Cambrex Bio Science Rockland Inc., ME, USA), transferred to Hybond-XL (GE Healthcare, UK) for overnight, hybridized with ^{32}P-labeled probes of $(CTG)_{10}$ oligonucleotide at 65°C for overnight, and detected using BAS2500 (Fuji Film, Japan). By using genomic DNA from a CDM patient with known CTG repeat number, we confirmed that this PCR-based method can detect the corresponding size of the CTG repeats using genomic DNA. For mutation screening of *ACTA1* and *TPM3*, all exons and their flanking intronic regions were amplified by PCR and directly sequenced by an ABI PRISM 3100 automated sequencer (Applied Biosystems). Primer sequences are listed in the Supplemental Table.

Statistical analyses

All data are presented as means ± SD. Comparisons among groups were done by using Student's t test and analysis of variance (ANOVA) as appropriate. Statistical significance was considered when p value was less than 0.05.

Results

Genetic analyses

By using triplet repeat primed PCR, expanded CTG repeats in *DMPK* were detected in 4 of 28 (14%) unrelated patients who were pathologically diagnosed as CFTD (Figs. 1, 2a). This diagnosis of CDM was further confirmed by Southern

blotting analysis, wherein all four patients had more than 1,000 CTG repeats (Fig. 2b). We also identified three heterozygous *ACTA1* mutations (p.Gly48Cys, p.Leu221-Pro, and p.Pro332Ser) in four unrelated CFTD patients. Two mutations of p.Leu221Pro and p.Pro332Ser have already been reported [8], whereas the p.Gly48Cys mutation observed in two patients was a novel one. The Gly48 is a highly conserved amino acid among several species. Two unrelated CFTD patients had the same heterozygous mutation p.Arg168Cys in *TPM3*, which was previously reported in CFTD patients [4].

Clinical findings

We compared the clinical findings among 4 CFTD patients with CTG expansion and 6 CFTD patients with *ACTA1* or *TPM3* mutations, and compared the clinical features with 20 patients genetically confirmed as CDM (Table 1). In terms of family history, none of the four CFTD patients with CTG expansion had a positive family history. This is in stark contrast with the typical picture in CDM patients, as all of them had at least one symptomatic family member. Hydramnios and premature delivery were seen in more than 50% of the CFTD patients with CTG expansion and CDM, but none of CFTD patients with *ACTA1* or *TPM3* mutations. Hypotonia and respiratory insufficiency at birth were seen in all groups except for two patients with *TPM3* mutation.

Muscle pathological findings

As muscle pathology can have drastic changes according to the gestational age of infantile patients, we adjusted the age by setting the full-term day (37 weeks of gestation) as putative birthday. After adjustment, the age at biopsy of the CDM patients ranged from −7 to 43 weeks, and those of the four CFTD patients with CTG expansion were from 21 to 42 weeks.

Congenital fiber type disproportion is defined as a congenital myopathy wherein FSD is higher than 12%, but with no associated structural abnormalities within the myofibers [2]. In this study, FSD in CDM, CFTD with CTG expansion, CFTD with *ACTA1* mutation, and CFTD with *TPM3* mutation was calculated to be 7.2 ± 6.8% (mean ± SD), 23.0 ± 5.0, 47.5 ± 4.0, and 52.0 ± 9.9%, respectively (Fig. 3). FSD was significantly ($p < 0.05$) higher in CFTD with *ACTA1* or *TPM3* mutations as compared to the CFTD patients with CTG expansion and CDM.

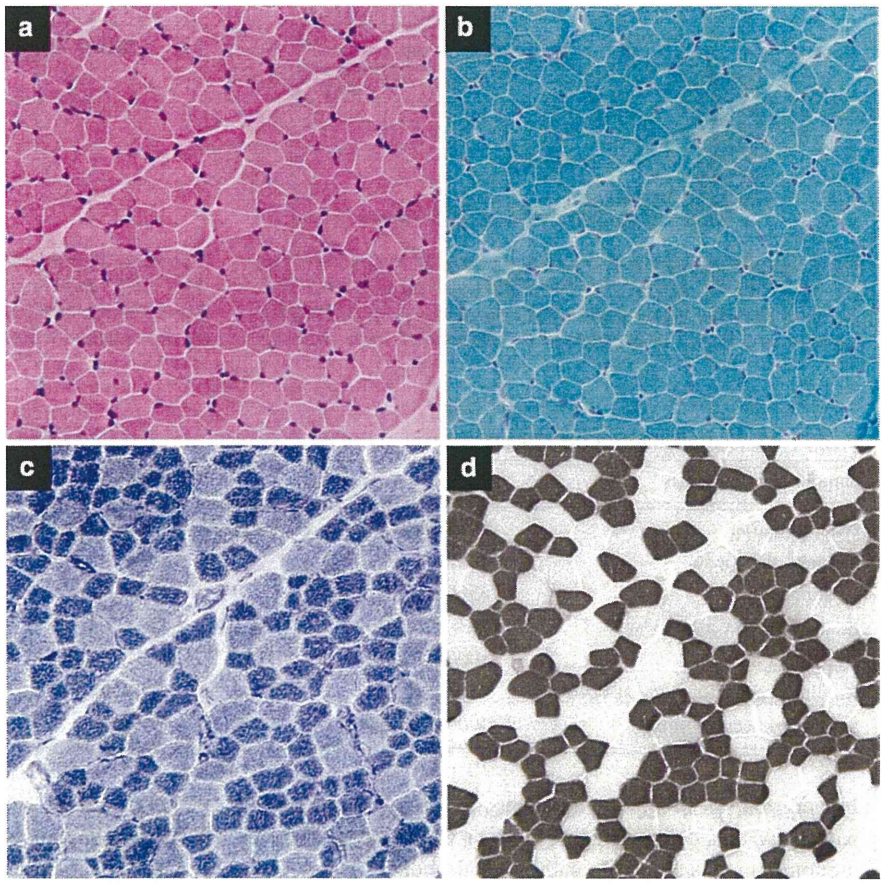

Fig. 1 Muscle pathology of a 42-week-old CFTD patient with CTG expansion. **a** Hematoxylin and eosin, **b** modified Gomori trichrome, **c** NADH-TR, and **d** ATPase (pH 4.4) stain. Type 1 fiber atrophy (FSD [(mean type 2 fiber diameter) − (mean type 1 fiber diameter)/mean type 2 fiber diameter × 100] = 26%), type 1 fiber predominance (65%), and only 1% of type 2C fibers with no peripheral halo is seen. *Bar* 50 μm

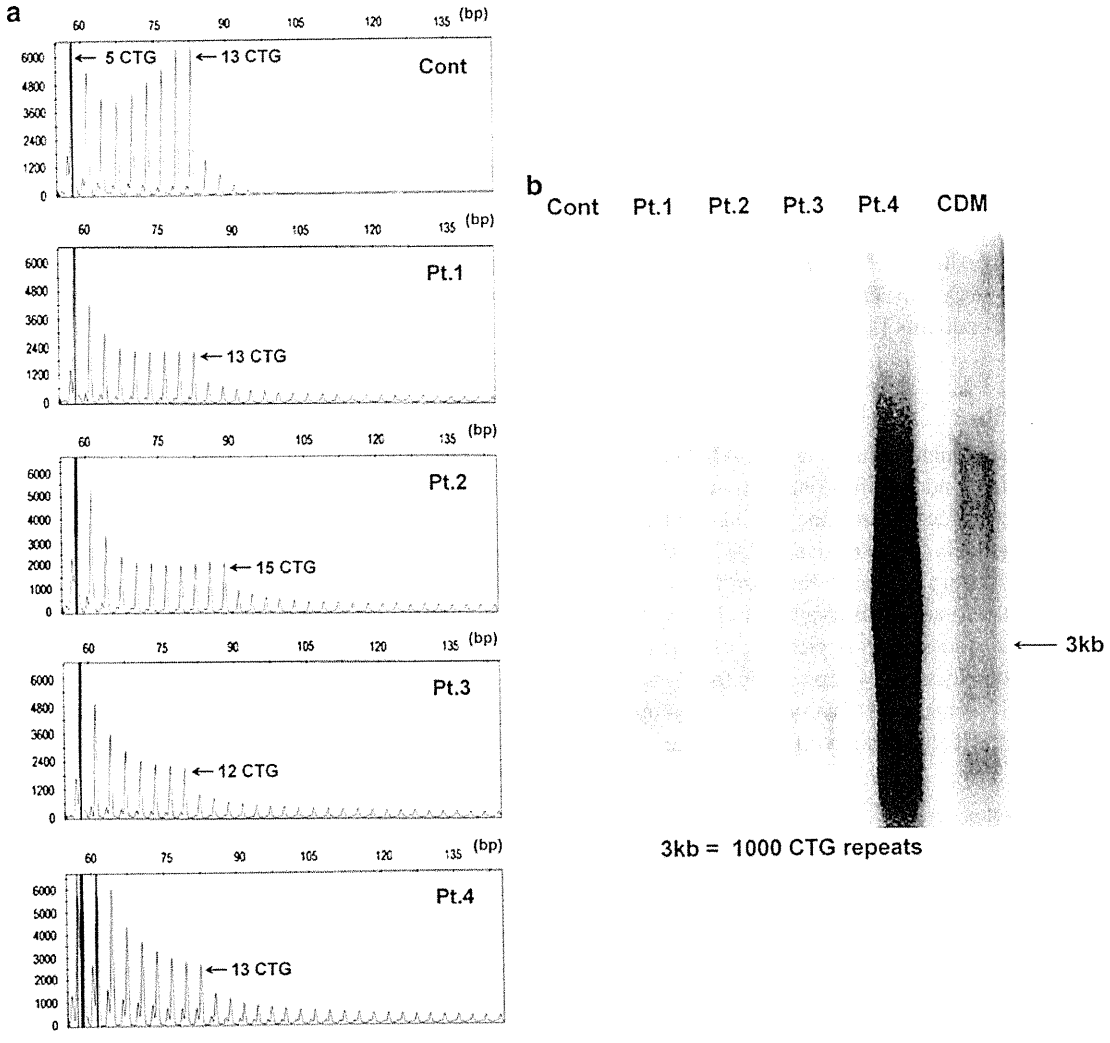

Fig. 2 Genetic analyses. **a** Triplet repeat primed PCR. Control (*Cont*) has 5 and 13 CTG repeats. The four CFTD patients (Pt.1, Pt.2, Pt.3, and Pt.4) have the ladder pattern that represents a large CTG allele together with higher peaks that show normal-sized allele (*arrows*). **b** Southern blotting analysis using PCR products. Four CFTD patients (Pt.1, Pt.2, Pt.3, and Pt.4) and one genetically confirmed CDM showed smear band larger than 3 kb corresponding to 1,000 CTG repeats, whereas a control (*Cont*) has no detectable band

Table 1 Clinical summary of the patients

Pathological diagnosis	CDM	CFTD	CFTD	CFTD
Gene mutation	CTG expansions in *DMPK*	CTG expansions in *DMPK*	*ACTA1*	*TPM3*
Number of patients	20	4	4	2
Hydramnios	65% (13/20)	50% (2/4)	0% (0/4)	0% (0/2)
Premature delivery (<37w)	50% (10/20)	50% (2/4)	0% (0/4)	0% (0/2)
Hypotonia at birth	100% (20/20)	100% (4/4)	100% (4/4)	0% (0/2)
Respiratory insufficiency at birth	95% (19/20)	75% (3/4)	75% (3/4)	0% (0/2)
Symptoms seen in family	100% (20/20)	0% (0/4)	0% (0/4)	0% (0/2)

In addition to FSD, we also checked other features in pathology that define either CFTD or CDM. Type 1 fiber predominance is a notable pathological finding observed in CFTD, and all our CFTD patients, including those with CTG expansion, showed type 1 fiber predominance. The mean composition of type 1 fibers in CDM, CFTD with

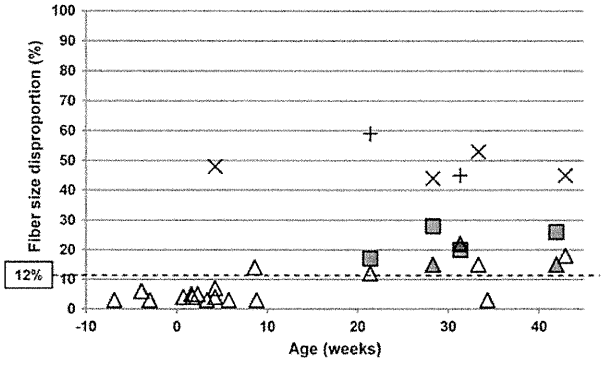

Fig. 3 Fiber size disproportion (*FSD*) of each patient. CFTD with CTG expansion (*filled square*; $N = 4$), CDM (*open triangle*; $N = 17$), CDM with similar pathological findings to CFTD (*filled triangle*; $N = 3$), CFTD with *ACTA1* mutations (*multi symbol*; N = 4), and CFTD with *TPM3* mutations (*plus*; $N = 2$). *Dot line* at 12% of FSD is the lowest FSD by the definition of CFTD

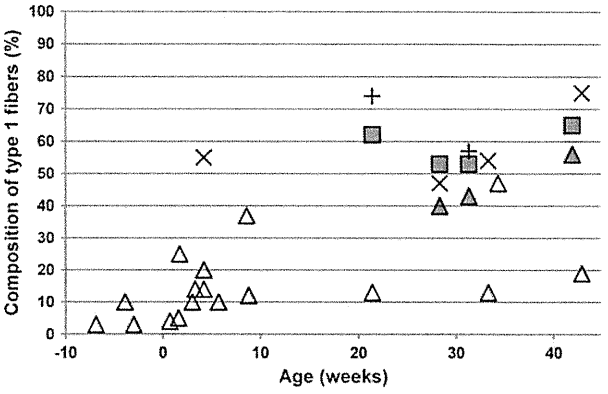

Fig. 4 Composition of type 1 fibers in each patient. *Filled square* CFTD with CTG expansion, *open triangle* CDM, *filled triangle* CDM with similar pathological findings to CFTD, *multi symbol* CFTD with *ACTA1* mutations, and *plus* CFTD with *TPM3* mutations

CTG expansion, and CFTD with *ACTA1* or *TPM3* mutations was 19.6 ± 16.3, 58.2 ± 6.2, 57.8 ± 2.0, and 65.5 ± 12.0%, respectively (Fig. 4). On the other hand, the presence of numerous immature type 2C fibers with peripheral halo is a characteristic finding in CDM. A markedly increased number of type 2C fibers were actually observed in CDM especially in patients younger than 10 weeks of adjusted age (Fig. 5). The frequency of type 2C fibers was inversely correlated to age of patients, while the number of type 1 fibers was directly proportional to age of patients. In other words, type 2C fibers were increased among younger age, while type 1 fiber predominance is seen more among older patients. Peripheral halo was observed in 14 of 20 (70%) CDM patients even in a 43-week-old patient. In CFTD patients with CTG expansion, type 2C fibers accounted for less than 20% and in CFTD with *ACTA1* or *TPM3* mutations, only a few type 2C fibers were seen. No peripheral halo was seen in either group. The increased number of fibers with internally located nuclei is another characteristic pathological finding of myotonic dystrophy. In our series, fibers containing internal nuclei were variably increased up to 26% in CDM patients, whereas less than 2% of fibers contained internal nuclei in the CFTD patients with CTG expansion or mutation in *ACTA1* or *TPM3*. The number of the fibers with internal nuclei is relatively correlated to the number of immature fibers in CDM, which may reflect immaturity of the fibers as described previously [6, 11].

Of the 20 CDM patients, 3 showed pathological findings similar to CFTD with CTG expansion. The ages of these three patients were 29, 32 and 42 weeks, respectively. FSD was 15–21%, with less than 20% of type 2C fibers and no peripheral halo. In these patients, the clinical diagnosis of CDM was made based upon the presence of the symptomatic family member.

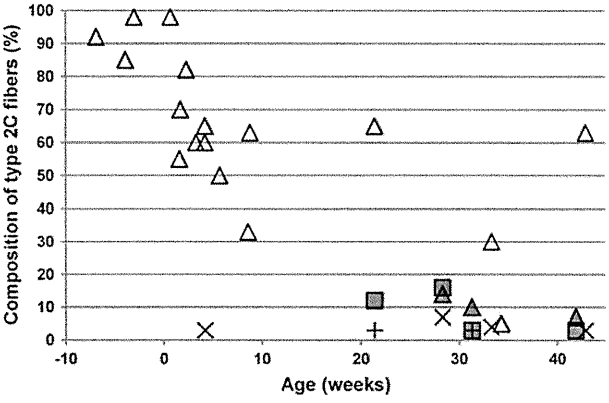

Fig. 5 Composition of type 2C fibers in each patient. *Filled square* CFTD with CTG expansion, *open triangle* CDM, *filled triangle* CDM with similar pathological findings to CFTD, *multi symbol* CFTD with *ACTA1* mutations, and *plus* CFTD with *TPM3* mutations

Discussion

In this study, we identified 4 of 28 patients (14%) who have CTG expansion in *DMPK* but were pathologically diagnosed as CFTD. Clinical symptoms of CFTD and CDM are quite similar during neonatal stage, including hypotonia and respiratory insufficiency. However, most of CDM patients are readily diagnosed by the presence of symptomatic family members, typically the mother. In fact, all CDM patients in our series had symptomatic family members and 75% of the mothers had the diagnosis of myotonic dystrophy. In contrast, no notable clinical symptoms were recorded in the mother of the CFTD patients with CTG expansion, and we could not examine the repeat size of the mothers. No marked difference in the size of CTG repeats was seen between CFTD patients with CTG expansion and CDM.

Among the CDM patients we examined, three patients showed pathological findings similar to those observed in CFTD with CTG expansion. They showed a small number of type 2C fibers, no peripheral halo, and hypotrophy of type 1 fibers (FSD >15%). The diagnosis of CDM was done from the typical clinical symptoms of myotonic dystrophy observed in the family member. Interestingly the ages of these three patients were over 29 weeks. Consistently, the ages of the patients who have CFTD with CTG expansion ranged from 21 to 42 weeks. These results suggest that CFTD pathology may be seen in this age range of CDM patients.

We identified four patients with mutations in *ACTA1* and two in *TPM3*. FSD in these patients was over 45% and significantly higher than that observed in CFTD with CTG expansion. This finding is also consistent with a previous report of CFTD patients with *TPM3* mutations whose muscle showed higher than 50% of FSD [4]. From these results, CDM should be considered for the patients whose muscle shows CFTD with FSD lower than 40%. In our series, only 4 (14%) and 2 (7%) of 28 patients had the mutations respectively in *ACTA1* and *TPM3*, leaving 18 (65%) patients still genetically uncharacterized and suggesting that defects in these genes may not be the major causes of CFTD in Japan. Further studies are necessary to elucidate such causes.

Acknowledgments We thank Dr. May Christine V. Malicdan (National Institute of Neuroscience, NCNP) for reviewing the manuscript. This study was supported by: the a Grant-in-Aid for Scientific Research and a Grain-in-aid for Exploratory Research from Japan Society for the Promotion of Science; by Research on Psychiatric and Neurological Diseases and Mental Health of Health Labour Sciences Research Grant and the Research Grant (20B-12, 20B-13) for Nervous and Mental Disorders from the Ministry of Health, Labour, and Welfare; by Research on Health Sciences focusing on Drug Innovation from the Japanese Health Sciences Foundation; and by the Program for Promotion of Fundamental Studies in Health Sciences of the National Institute of Biomedical Innovation (NIBIO).

References

1. Brook JD, McCurrach ME, Harley HG et al (1992) Molecular basis of myotonic dystrophy: expansion of a trinucleotide (CTG) repeat at the 3′ end of a transcript encoding a protein kinase family member. Cell 69:385
2. Clarke NF, North KN (2003) Congenital fiber type disproportion—30 years on. J Neuropathol Exp Neurol 62:977–989
3. Clarke NF, Kidson W, Quijano-Roy S et al (2006) SEPN1: associated with congenital fiber-type disproportion and insulin resistance. Ann Neurol 59:546–552
4. Clarke NF, Kolski H, Dye DE et al (2008) Mutations in TPM3 are a common cause of congenital fiber type disproportion. Ann Neurol 63:329–337
5. Fu YH, Pizzuti A, Fenwick RG Jr et al (1992) An unstable triplet repeat in a gene related to myotonic muscular dystrophy. Science 255:1256–1258
6. Harper PS, Monckton DG (2004) Myotonic dystrophy. In: Engel AG, Franzini-Armstrong C (eds) Myology, 3rd edn. McGraw-Hill, New York, pp 1039–1076
7. The International Myotonic Dystrophy Consortium (IDMC) (2000) New nomenclature and DNA testing guidelines for myotonic dystrophy type 1 (DM1). Neurology 54:1218–1221
8. Laing NG, Clarke NF, Dye DE et al (2004) Actin mutations are one cause of congenital fibre type disproportion. Ann Neurol 56:689–694
9. Mahadevan M, Tsilfidis C, Sabourin L et al (1992) Myotonic dystrophy mutation: an unstable CTG repeat in the 3′ untranslated region of the gene. Science 255:1253–1255
10. Surh LC, Mahadevan M, Korneluk RG (1998) Analysis of trinucleotide repeats in myotonic dystrophy. In: Dracopoli NC, Haines JL, Korf BR, Morton CC et al (eds) Current protocols in human genetics, vol 2. Wiley, New York, unit 9.6.1-13
11. Tanabe Y, Nonaka I (1987) Congenital myotonic dystrophy. Changes in muscle pathology with ageing. J Neurol Sci 77:59–68
12. Warner JP, Barron LH, Goudie D et al (1996) A general method for the detection of large CAG repeat expansions by fluorescent PCR. J Med Genet 33:1022–1026

JCS ePress online publication date 27 October 2010

Specific phosphorylation of Ser458 of A-type lamins in *LMNA*-associated myopathy patients

Hiroaki Mitsuhashi[1], Yukiko K. Hayashi[1,*], Chie Matsuda[2], Satoru Noguchi[1], Shuji Wakatsuki[3], Toshiyuki Araki[3] and Ichizo Nishino[1]

[1]Department of Neuromuscular Research, National Institute of Neuroscience, National Center of Neurology and Psychiatry, 4-1-1 Ogawa-higashi, Kodaira, Tokyo 187-8502, Japan
[2]Neuroscience Research Institute, AIST, Central 6, Tsukuba, Ibaraki 305-8566, Japan
[3]Department of Peripheral Nervous System Research, National Institute of Neuroscience, National Center of Neurology and Psychiatry, Kodaira, Tokyo 187-8502, Japan
*Author for correspondence (hayasi_y@ncnp.go.jp

Accepted 9 August 2010
Journal of Cell Science 123, 3893-3900

doi:10.1242/jcs.072157

Summary

Mutations in *LMNA*, which encodes A-type nuclear lamins, cause various human diseases, including myopathy, cardiomyopathy, lipodystrophy and progeria syndrome. To date, little is known about how mutations in a single gene cause a wide variety of diseases. Here, by characterizing an antibody that specifically recognizes the phosphorylation of Ser458 of A-type lamins, we uncover findings that might contribute to our understanding of laminopathies. This antibody only reacts with nuclei in muscle biopsies from myopathy patients with mutations in the Ig-fold motif of A-type lamins. Ser458 phosphorylation is not seen in muscles from control patients or patients with any other neuromuscular diseases. In vitro analysis confirmed that only lamin A mutants associated with myopathy induce phosphorylation of Ser458, whereas lipodystrophy- or progeria-associated mutants do not. We also found that Akt1 directly phosphorylates Ser458 of lamin A with myopathy-related mutations in vitro. These results suggest that Ser458 phosphorylation of A-type lamins correlates with striated muscle laminopathies; this might be useful for the early diagnosis of *LMNA*-associated myopathies. We propose that disease-specific phosphorylation of A-type lamins by Akt1 contributes to myopathy caused by *LMNA* mutations.

Key words: Laminopathy, A-type lamins, EDMD, LGMD1B, Akt

Introduction

Mutations in *LMNA* cause at least 13 human hereditary diseases, collectively termed 'laminopathies'. These include striated muscle diseases, such as autosomal dominant and recessive forms of Emery-Dreifuss muscular dystrophy (AD/AR-EDMD) (Bonne et al., 1999; Raffaele Di Barletta et al., 2000), limb-girdle muscular dystrophy type 1B (LGMD1B) (Muchir et al., 2000), *LMNA*-related congenital muscular dystrophy (L-CMD) (Quijano-Roy et al., 2008) and dilated cardiomyopathy (Fatkin et al., 1999), and other conditions including Hutchinson-Gilford progeria syndrome (HGPS) (De Sandre-Giovannoli et al., 2003; Eriksson et al., 2003), atypical Werner syndrome (Chen et al., 2003), mandibuloacral dysplasia (MAD) (Novelli et al., 2002) and Dunnigan-type familial partial lipodystrophy (FPLD) (Shackleton et al., 2000). It is still not clear how mutations in *LMNA* cause such a wide variety of tissue-specific degenerative diseases, although A-type lamins are ubiquitously expressed.

A-type lamins, of which lamin A and lamin C are the predominant somatic cell isoforms, are type V intermediate filament proteins that form the nuclear lamina, a meshwork on the nucleoplasmic side of the inner nuclear membrane (Burke and Stewart, 2002; Capell and Collins, 2006). Like all intermediate filament proteins, lamins have a tripartite structure consisting of an N-terminal head, a central coiled-coil rod domain and a large globular C-terminal tail. The C-terminal tail domain has an immunoglobulin-like fold (Ig-fold) motif (residues 436–544); these motifs are known to be involved in protein–protein interactions (Dechat et al., 2000; Lee et al., 2001; Sakaki et al., 2001; Zastrow et al., 2006; Zastrow et al., 2004). In addition to their primary role in providing mechanical support for nuclear membranes to maintain nuclear shape and size (Goldman et al., 2004), lamin filaments are believed to play important roles in mitosis (Tsai et al., 2006), chromatin organization (Glass et al., 1993; Park et al., 2009; Taniura et al., 1995), transcription (Spann et al., 2002) and DNA replication (Moir et al., 2000; Spann et al., 1997).

According to the PhosphoSite database (http://www.phosphosite.org/), more than 30 phosphorylation sites in human A-type lamins have been reported. Phosphorylation of Thr19, Ser22 and Ser392 leads to depolymerization of lamin filaments during nuclear envelope breakdown in mitosis and meiosis (Haas and Jost, 1993; Heald and McKeon, 1990; Peter et al., 1990; Ward and Kirschner, 1990), but the physiological importance of the phosphorylation of other sites in A-type lamins is largely unknown. Previously, Cenni et al. reported that N-terminal phosphorylation of lamin A was specifically decreased in the muscles of four AD-EDMD or LGMD1B patients (Cenni et al., 2005), implicating unidentified lamin A phosphorylation sites in the pathomechanism of AD-EDMD and LGMD1B.

Here, we produced site- and phosphorylation-state-specific antibodies against human A-type lamins, and found that the antibody against phosphorylated Ser458 specifically detects myopathy patients who have mutations within the Ig-fold motif of the C-terminal tail domain of A-type lamins. In vitro expression analysis revealed that Ser458 phosphorylation was specific to myopathy-causing *LMNA* mutations, because it was not detected in cells with mutations related to FPLD or progeria. These results imply that Ser458 phosphorylation might have particular roles in the pathomechanism of *LMNA*-associated myopathy.

Journal of Cell Science

Results

Ser458 phosphorylation of A-type lamins in the muscles of *LMNA*-associated myopathy patients

To examine the phosphorylation state of A-type lamins, we raised rabbit polyclonal antibodies against three phosphorylated A-type lamin peptides – Ser5-*P*, Thr416-*P* and Ser458-*P* (Fig. 1A); these serine and threonine residues are well conserved between species. We performed immunohistochemistry of muscle specimens from 17 genetically confirmed *LMNA*-associated myopathy patients, including AD-EDMD, LGMD1B and L-CMD patients.

Using the purified anti-phospho-Ser458 antibody (anti-Ser458-*P* Ab), we found clear nuclear staining in muscles from patients with *LMNA*-associated myopathies, but not in control muscles (Fig. 1Ba–d). Notably, strong immunoreaction to anti-Ser458-*P* Ab was observed in all eight patients carrying a mutation within the Ig-fold motif, whereas the remaining nine patients with mutations outside of the Ig-fold domain showed barely detectable nuclear staining (Table 1). Ser458 is an evolutionarily highly conserved residue within the Ig-fold motif (amino acids 436–544) of A-type lamins (supplementary material Fig. S1A). Anti-Ser458-*P* Ab staining was independent of patient age and sex, and independent of the nature or severity of myopathy, because positive staining for Ser458-*P* was seen in AD-EDMD, LGMD1B, L-CMD and infantile inflammatory myopathy (IIM) cases.

Positive staining with the anti-Ser458-*P* antibody was detected in myonuclei [both peripheral and centrally located (Fig. 1Bb,d,e,g)], vascular endothelial and smooth muscle cell nuclei (Fig. 1Bi), and the nuclei of unidentified cells outside the basal lamina (Fig. 1Bf,h). Double staining with anti-Ser458-*P* and anti-Pax7 antibodies also revealed positive staining in nuclei of satellite cells in patient muscles (Fig. 1Bj–l). Double staining with antibodies for Ser458-*P* and pan-A-type lamins showed that 69.0±7.3% of nuclei were immunostained in patient muscles with mutations in the Ig-fold domain. These results suggest that the Ser458 phosphorylation might be common in *LMNA*-associated myopathy patients with mutations in the Ig-fold domain of A-type lamins.

Consistent with the immunohistochemistry results, the anti-Ser458-*P* Ab detected two main bands at 70 kDa and 65 kDa, corresponding to lamins A and C, respectively, in muscle from laminopathy patients, but not in unaffected control muscle (Fig. 2).

No Ser458 phosphorylation of A-type lamins in patients with other neuromuscular disorders

To determine whether Ser458 phosphorylation is specific to *LMNA*-associated myopathy, we immunostained muscle specimens from patients with other neuromuscular diseases, including X-linked EDMD (X-EDMD (Fig. 3c,d), Duchenne muscular dystrophy (DMD) (Fig. 3e,f), Becker muscular dystrophy (BMD) (Fig. 3g,h), LGMD2A (Fig. 3i,j), LGMD2B (Fig. 3k,l), sporadic inclusion body myositis (sIBM) (Fig. 3m,n), idiopathic polymyositis (PM) (Fig. 3o,p) and myotonic dystrophy type 1 (MyD1) (Fig. 3q,r). As shown in Fig. 3, Ser458 phosphorylation was only observed in

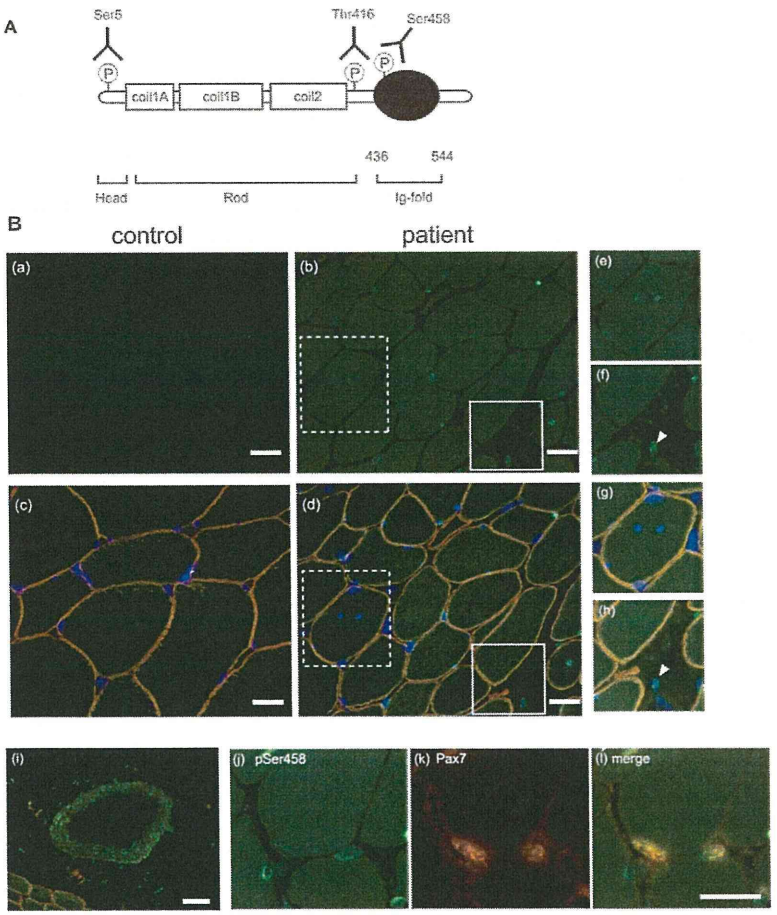

Fig. 1. Ser458 of A-type lamins is specifically phosphorylated in muscles from *LMNA*-associated myopathy patients. (**A**) Schematic model of three antibodies against phosphorylated A-type lamins (Ser5-*P* Ab, Thr416-*P* Ab and Ser458-*P* Ab). Amino acid residues 436–544 form an Ig-fold structure in the C-terminal globular tail domain. (**B**) Immunohistochemistry of human muscles with anti-Ser458-*P* antibody. Nuclei in patient muscle (P11) show positive staining for anti-Ser458-*P* antibody (b,d), whereas no positive nuclear staining is seen in control muscle (a,c). Anti-Ser458-*P* Ab is green and anti-merosin antibody is red. (c,d) Merged images. Blue is DAPI staining. (e,f) Magnified images of boxes in b. (g,h) Magnified images of boxes in d. Note that centrally placed nuclei and nuclei in non-muscle cells outside of the basal lamina (arrowheads) are immunostained with anti-Ser458-*P* Ab. (i) Nuclei in blood vessels in the patient muscle (P14) are also immunostained with anti-Ser458-*P* Ab. (j–l) Double staining of *LMNA*-associated myopathy patient muscle (P12) with anti-Ser458-*P* Ab (j) and anti-pax7 (k) reveals colocalization (l), indicating the occurrence of Ser458 phosphorylation in the patient satellite cells. Scale bars: 20 μm.

Table 1. Summary of anti-Ser458-*P* antibody staining of A-type lamins from 17 *LMNA*-associated myopathy patients

Patient	Age	Sex	Clinical diagnosis	*LMNA* mutation	Domain	Anti-Ser458-*P* Ab
P1	3y 11m	F	LGMD1B	p.R28Q	Head	–
P2	2y 1m	F	IIM	p.K32 deletion	Head	–
P3	1y	M	IIM	p.R41S	Rod	–
P4	1y 6m	F	L-CMD	p.R41C	Rod	–
P5	2y 8m	F	LGMD1B	p.R249Q	Rod	–
P6	5y 3m	F	LGMD1B	p.S303P	Rod	–
P7	47y	M	LGMD1B	p.K311R	Rod	–
P8	2y 5m	M	IIM	p.E358K	Rod	–
P9	1y 9m	F	L-CMD	p.E444_D446 duplication	Tail (Ig fold)	+
P10	11y 1m	F	EDMD	p.R453W	Tail (Ig fold)	+
P11	4y 5m	F	LGMD1B	p.R453W	Tail (Ig fold)	+
P12	4y	F	LGMD1B	p.R453W	Tail (Ig fold)	+
P13	5y	F	IIM	p.N456H	Tail (Ig fold)	+
P14	7y 2m	M	LGMD1B	p.W514R	Tail (Ig fold)	+
P15	25y	F	LGMD1B	p.R527P	Tail (Ig fold)	+
P16	2y 11m	M	LGMD1B	p.T528K	Tail (Ig fold)	+
P17	52y	F	LGMD1B	p.V547X	Tail	–

patients with *LMNA*-associated myopathy (Fig. 3a,b), but not with other muscle diseases such as X-EDMD (Fig. 3c,d), which is clinically indistinguishable from AD-EDMD. This result suggests that Ser458 phosphorylation is likely to be specific to *LMNA* mutations.

In contrast to the anti-Ser458-*P* antibody, the anti-Ser5-*P* antibody strongly recognized nuclei in all human muscles examined, with no disease or mutation specificity. The anti-Thr416-*P* antibody showed very weak staining in nuclei, with no difference between control and patients (supplementary material Fig. S1B,C).

Ser458 phosphorylation of A-type lamins in AD-EDMD patient fibroblasts

Because Ser458 phosphorylation of A-type lamins was also observed in the nuclei of non-muscle tissues (Fig. 1B), we performed immunocytochemistry using cultured skin fibroblasts from one unaffected person and two AD-EDMD patients with either a Leu102Pro mutation in the rod domain or a Arg453Trp mutation in the Ig-fold domain. Anti-Ser458-*P* Ab staining was observed only in the fibroblasts with the Arg453Trp mutation, but not in control and Leu102Pro mutant fibroblasts (Fig. 4). All nuclei in the Arg453Trp fibroblasts were immunopositive, implying that Ser458 phosphorylation might be independent of the cell cycle. These results suggested that Ser458 phosphorylation requires mutations in the Ig-fold motif of A-type lamins and can occur in non-muscle cells.

Ser458 phosphorylation of A-type lamins in transfected cells

Next, we analyzed the specificity of anti-Ser458-*P* Ab to phosphorylation by examining ectopically expressed FLAG-tagged lamin A and FLAG-tagged Arg453Trp mutant lamin A, which is the most common mutation in *LMNA*-associated myopathy. Anti-Ser458-*P* Ab strongly detected the ectopic FLAG–Arg453Trp mutant in a western blot analysis and slightly detected even wild-type lamin A when overexpressed in COS-7 cells (Fig. 5A). Importantly, alkaline phosphatase treatment reduced the immunoreactivity of anti-Ser458-*P* Ab to background levels (Fig. 5A, IP), strongly suggesting that anti-Ser458-*P* Ab specifically recognizes the phosphorylation of Ser458 of mutant A-type lamins.

To further verify the specificity of anti-Ser458-*P* Ab, we transfected C2 myoblasts to express FLAG-tagged wild-type lamin A or FLAG-tagged lamin A bearing either the Ser458Ala or Arg453Trp mutation, or both mutations (FLAG–Arg453Trp/Ser458Ala) (Fig. 5B). Anti-Ser458-*P* Ab immunostained only the nuclei that expressed FLAG–Arg453Trp, whereas the nuclei that expressed FLAG–Arg453Trp/Ser458Ala were barely detectable with anti-Ser458-*P* Ab. These results confirmed the specificity of anti-Ser458-*P* Ab to Ser458 phosphorylation.

Ser458 phosphorylation is not detected in other laminopathies

As several mutations associated with FPLD, MAD and HGPS are known to be located within the Ig-fold motif of A-type lamins, we wanted to find out whether Ser458 phosphorylation also occurs in such mutants. We therefore transfected lamin A mutants associated with AD-EDMD (Leu140Pro, Arg453Trp, Arg527Pro, Leu530Pro) (Bonne et al., 1999; Boriani et al., 2003), LGMD1B (Tyr481His) (Kitaguchi et al., 2001), FPLD (Gly465Asp, Arg482Trp, Lys486Asn) (Shackleton et al., 2000; Speckman et al., 2000), MAD (Arg471Cys and Arg527His) (Cao and Hegele, 2003; Novelli et al., 2002) and HGPS (Met540Thr) (Verstraeten et al., 2006) into C2 myoblasts, and checked immunoreactivity with anti-Ser458-*P* Ab. As expected, Ig-fold mutants Arg453Trp, Arg527Pro, Leu530Pro and Tyr481His were detected by anti-Ser458-*P* antibody (Fig. 6). By contrast, rod domain mutant Leu140Pro formed intranuclear foci that were not detected by anti-Ser458-*P* Ab. Interestingly, lamin A mutations associated with FPLD (Gly465Asp, Arg482Trp, Lys486Asn), MAD (Arg471Cys, Arg527His) and

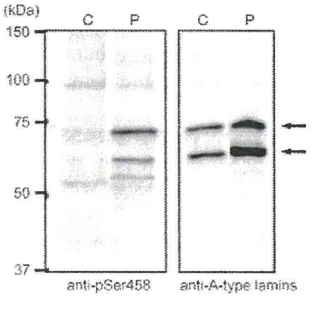

Fig. 2. Western blot analysis of patient muscle with anti-Ser458-*P* Ab. Anti-Ser458-*P* Ab specifically recognizes proteins of ~70 kDa and 65 kDa, corresponding to lamin A and lamin C, respectively. Representative data from patient 13 (P13) are shown. C: control. P: patient.

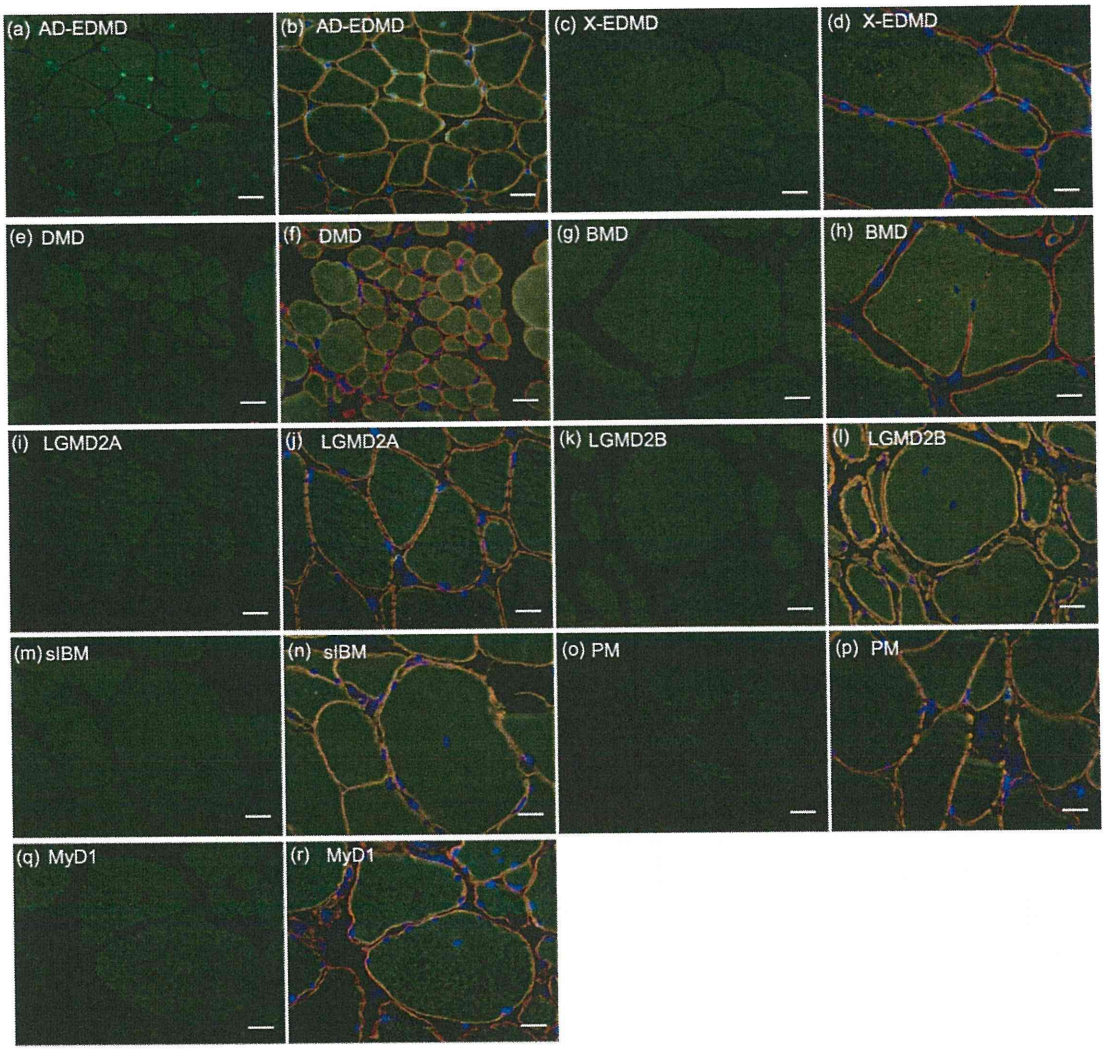

Fig. 3. Immunohistochemical analysis of other neuromuscular diseases. Muscles from myopathic patients were immunostained with anti-Ser458-*P* Ab (green) and anti-merosin (red). (**a**,**b**) AD-EDMD with Arg453Trp mutation in *LMNA* (P11). (**c**,**d**) X-EDMD. (**e**,**f**) DMD. (**g**,**h**) BMD. (**i**,**j**) LGMD2A. (**k**,**l**) LGMD2B. (**m**,**n**) sIBM. (**o**,**p**) PM. (**q**,**r**) MyD1. (b,d,f,h,j,l,n,p,r) Merged images. Nuclei were stained with DAPI (blue). Scale bars: 20 μm.

HGPS (Met540Thr), which are all located in the Ig-fold motif, were negative for anti-Ser458-*P* Ab. These results suggested that Ser458 in A-type lamins might be specifically phosphorylated in laminopathies related to myopathy, but not in other laminopathies even with mutations in the Ig-fold domain.

Akt1 directly phosphorylates Ser458 of lamin A

The sequence around Ser458 contains the Akt consensus sequence RxRxxS. To test whether Akt phosphorylates Ser458 of lamin A, COS-7 cells were co-transfected with wild-type Akt (wtAkt–HA) or myristoylated Akt (myrAkt–HA), which is regarded as a constitutively active form (Andjelkovic et al., 1997; Manning and Cantley, 2007), and FLAG-tagged lamin A constructs. The cell lysates were immunoprecipitated with FLAG M2 agarose and detected with anti-Ser458-*P* Ab. Coexpression of wtAkt–HA enhanced Ser458 phosphorylation of the Arg453Trp mutant; this signal became even stronger in cells co-transfected with myrAkt–HA (Fig. 7A). By contrast, only background levels of Ser458 phosphorylation were detected for wild-type lamin A and the double (Arg453Trp/Ser458Ala) mutant (Fig. 7A). The same results were obtained by co-transfection in C2 myotubes (supplementary material Fig. S2). To determine whether Ser458 phosphorylation is sensitive to the specific amino acid present at position Arg527, we co-transfected COS-7 cells with wtAkt–HA plus either the myopathy-causing Arg527Pro mutation or the MAD-causing Arg527His mutation of FLAG-tagged lamin A (Fig. 7B). Only background levels of Ser458 phosphorylation were detected with wild-type and His-substituted lamin A, suggesting specific recognition of myopathic Arg527Pro-mutated lamin A by Akt1.

To determine whether Akt1 directly phosphorylates Ser458 of lamin A, we performed an in vitro kinase assay using the purified C-terminal tail domain of lamin A (LA-T, amino acids 411–553) and a recombinant, constitutively active form of Akt1 (rAkt).

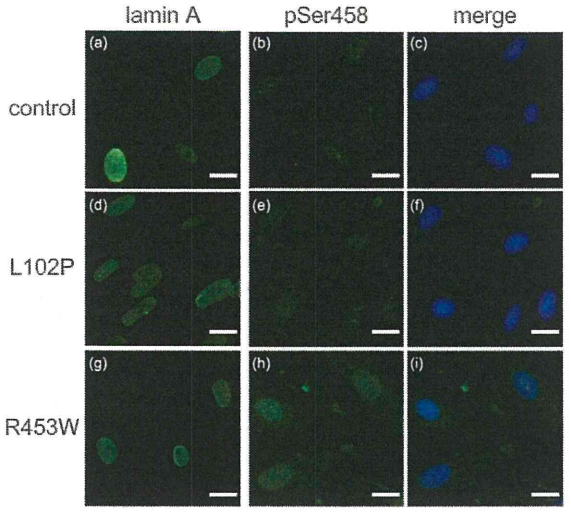

Fig. 4. Immunocytochemistry of human fibroblasts. Only fibroblasts from an AD-EDMD patient with an Arg453Trp mutation in the Ig-fold domain are detected with anti-Ser458-*P* Ab (h), whereas nuclear staining of cells from a control and an AD-EDMD patient with a Leu102Pro mutation is barely detectable (b,e). (**a**,**d**,**g**) Staining with anti-lamin A antibody, (**b**,**e**,**h**) staining with anti-Ser458-*P* Ab, (**c**,**f**,**i**) merged images of anti-Ser458-*P* Ab and DAPI. Scale bars: 20 μm.

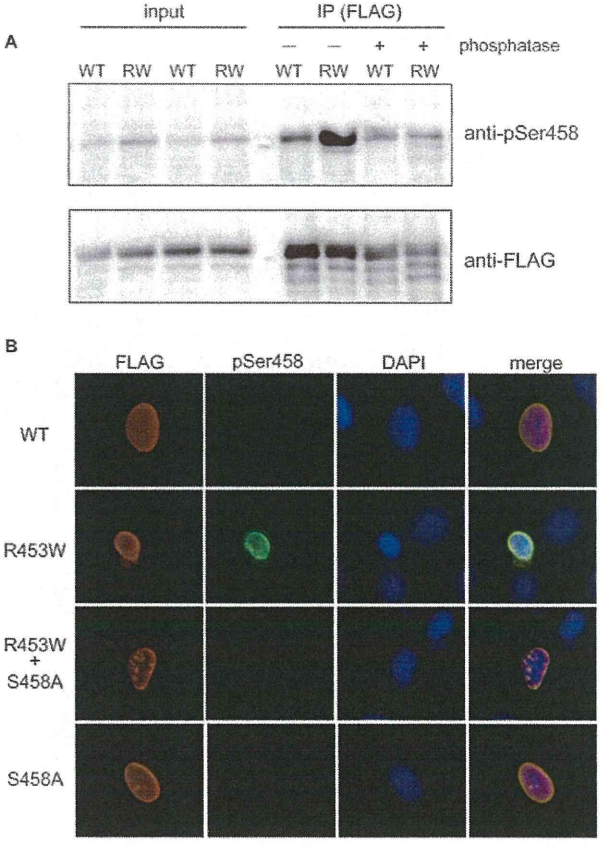

Fig. 5. Anti-Ser458-*P* Ab specifically recognizes the phosphorylation of Ser458 of lamin A. (A) Western blot analysis of transfected cells. FLAG-tagged lamin A constructs were overexpressed in COS-7 cells. The cell lysates were subjected to immunoprecipitation with anti-FLAG M2 antibody. The immunoprecipitates were incubated with (+) or without (–) calf intestine alkaline phosphatase, and then resolved by SDS-PAGE. WT: wild type, RW: Arg453Trp mutant. (**B**) Substitution of Ser458 to Ala diminishes the immunoreactivity of anti-Ser458-*P* against Arg453Trp mutant lamin A. Wild-type or mutant lamin A were overexpressed in C2 myoblasts, and then transfected cells were double immunostained with anti-FLAG Ab (red) and anti-Ser458-*P* Ab (green). Nuclei were stained with DAPI (blue).

Consistently, LA-T with the Arg453Trp mutation was phosphorylated by rAkt in vitro (Fig. 7C). rAkt failed to phosphorylate LA-T with Arg453Trp/Ser458Ala double mutations, indicating that Ser458 is a genuine Akt phosphorylation site. We conclude that Ser458 in lamin A is specifically phosphorylated by Akt1, even in non-muscle cells, when the Ig-fold domain bears mutations that cause myopathy; Ser458 is not phosphorylated when lamin A bears mutations, even in the Ig-fold, that cause disease in other tissues.

Discussion

For the first time, we have identified a disease-related phosphorylation site of A-type lamins using the antibody that specifically recognizes the phosphorylation of Ser458 of A-type lamins. Cenni et al. previously reported a monoclonal antibody, named SW2-30, that recognizes the phosphorylation of the N-terminal region of A-type lamins in normal muscles, but immunoreactions were barely detectable in myonuclei from AD-EDMD and LGMD1B patients (Cenni et al., 2005). The precise phosphorylation site was not determined, but the change in phosphorylation state between control and patients was the reverse of that seen with Ser458. In contrast to previously reported cell-cycle-specific phosphorylation (Heald and McKeon, 1990; Peter et al., 1990; Ward and Kirschner, 1990), Ser458 phosphorylation is independent of cell cycle, because the all nuclei in replicating fibroblasts from patients with the Arg453Trp mutation were immunopositive.

The early diagnosis of *LMNA*-associated myopathy is particularly important because the patients eventually develop severe cardiac problems with conduction defects, with high mortality (Bonne et al., 2003; Taylor et al., 2003). Because patients show a wide variety of clinicopathological features and recent research has revealed the spectrum of *LMNA*-associated myopathy to be broader than previously understood (Quijano-Roy et al., 2008), simple screening using disease-specific phospho-A-type lamin antibodies should be quite useful. Interestingly, the position of the mutation in *LMNA* is important for positive staining by anti-Ser458-*P* Ab (Table 1). About 30% of AD-EDMD and LGMD1B patients previously reported have the mutation within the Ig-fold motif (Leiden Muscular Dystrophy Pages; http://www.dmd.nl/). The Arg453Trp mutation, which is the most common mutation in AD-EDMD, is also located within this motif. Anti-Ser458-*P* antibody also detected the nuclei in skin fibroblasts and the vascular endothelial cells of patients, suggesting that skin biopsy, which is less invasive for the patient, might be used for the diagnosis.

We have revealed that Akt1 phosphorylates Ser458 of myopathy-related mutant lamin A. A recent study also reported that Ser404 of lamin A is phosphorylated by Akt (Cenni et al., 2008). Interestingly, Ser458 of wild-type lamin A was not phosphorylated by Akt1 even in vitro (Fig. 7C), suggesting that

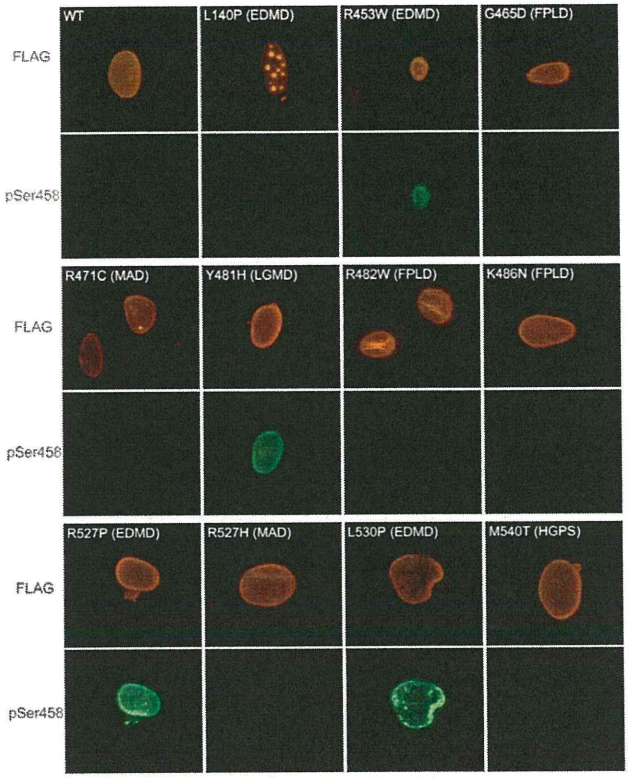

Fig. 6. Myopathy-specific phosphorylation of Ser458 of lamin A. Lamin A mutants that cause AD-EDMD, LGMD1B, FPLD, HGPS or MAD were overexpressed in C2 myoblasts. Transfected cells were double immunostained with anti-FLAG Ab (upper panel, red) and anti-Ser458-*P* Ab (lower panel, green).

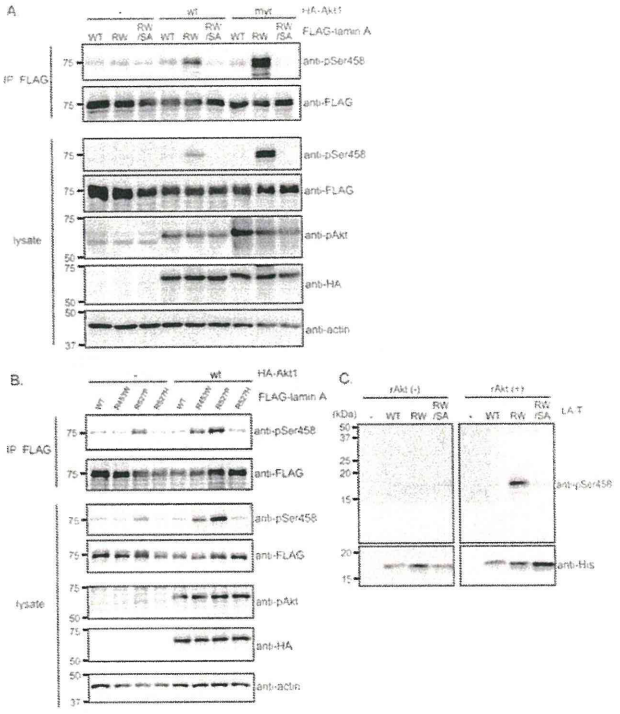

Fig. 7. Akt1 directly phosphorylates Ser458 of lamin A with myopathy-related mutations. (A) COS-7 cells were transfected with Akt–HA constructs (wtAkt–HA or myrAkt–HA) and FLAG–lamin A constructs (WT: wild type, RW: Arg453Trp mutant, RW/SA: Arg453Trp/Ser458Ala mutant) for 30 hours. FLAG–lamin A was immunoprecipitated (IP), then probed with anti-Ser458-*P* and anti-FLAG M2 antibodies. Whole-cell lysates were also probed with anti-phospho-Akt Ser473 (anti-pAkt), and anti-HA and anti-actin antibodies to confirm equivalent levels of expression. **(B)** COS-7 cells were transfected with FLAG–lamin A constructs alone or co-transfected with wtAkt–HA for 30 hours. FLAG–lamin A was immunoprecipitated, then immunoblotted as described above. **(C)** Purified His-tagged C-terminal tail domain of lamin A (LA-T) was phosphorylated in vitro in the presence (+) or absence (–) of recombinant active Akt (rAkt). The membranes were probed with anti-Ser458-*P* and anti-His tag antibodies.

Ser458 is buried in wild-type lamin A. Ser458 was found to be partly buried and structural studies have showed that the Arg453Trp mutation destabilizes the three-dimensional structure of the Ig-fold motif, whereas the mutations observed in FPLD (Arg482Trp and Arg482Gln) do not (Krimm et al., 2002). We propose that *LMNA* mutations that make Ser458 easily accessible to Akt1 phosphorylation predispose patients to muscle pathology.

It is nonetheless perplexing that EDMD and LGMD1B patients with mutations outside the Ig-fold domain have no detectable Ser458 phosphorylation. We speculate that mutations outside the Ig-fold motif might cause myopathy by different mechanisms, for example, by disrupting protein–protein interactions or lamin filament formation, because rod domain mutations such as Leu140Pro can disrupt polymerization and mislocalize lamins. Although further studies are needed to understand these mechanisms, antibodies that recognize Ser458-phosphorylated lamin A will be immediately useful for the differential diagnosis of a large fraction of *LMNA*-associated myopathies.

Materials and Methods

Clinical materials

All clinical materials used in this study were obtained for diagnostic purposes with informed consent. The studies were approved by the Ethical Committee of the National Center of Neurology and Psychiatry.

Mutation analysis

Genomic DNA was isolated from peripheral lymphocytes or muscle specimens using standard techniques. All *LMNA* exons and their flanking intronic regions were sequenced directly for all 17 patients using an ABI PRISM 3100 automated sequencer (PE Applied Biosystems, Foster City, CA). Primer sequences are shown in supplementary material Table S1.

Antibody production and purification

The following peptides for immunization were synthesized by MBL (Ina, Nagano, Japan). For phospho-A-type lamins: Ser5-*P* (Met-Glu-Thr-Pro-phosphoSer-Gln-Arg-Arg-Ala-Thr-Cys); Thr416-*P* (AcetylVal-phosphoThr-Lys-Lys-Arg-Lys-Leu-Glu-Cys); Ser458-*P* (Cys-Leu-Arg-Asn-Lys-phosphoSer-Asn-Glu-Asp-Gln-Ser). For non-phospho-A-type lamins: Ser5 (Met-Glu-Thr-Pro-Ser-Gln-Arg-Arg-Ala-Thr-Cys); Thr416 (AcetylVal-Thr-Lys-Lys-Arg-Lys-Leu-Glu-Cys); Ser458 (Cys-Leu-Arg-Asn-Lys-Ser-Asn-Glu-Asp-Gln-Ser).

To obtain the specific antibody for phospho-A-type lamins, rabbits were immunized with the phospho-peptides conjugated to keyhole limpet hemocyanin (KLH). Antisera were purified by affinity chromatography at 4°C. First, antisera were passed through HiTrap NHS-activated HP columns (GE Healthcare UK, Buckinghamshire, UK) coupled with non-phospho-A-type lamin peptides. Then, the flow-through fractions were collected. Next, the flow-through fractions were passed through the columns coupled with phospho-A-type lamin peptides. Antibodies were eluted with 0.15 M glycine HCl (pH 2.7), concentrated by Amicon ultra-4 (Millipore, Bedford, MA, USA) and dialyzed with PBS at 4°C overnight. Approximately 0.2 μg/μl of antibody was obtained.

Immunohistochemistry

Biopsied muscle specimens were frozen in isopentane cooled in liquid nitrogen. Serial frozen sections of 6 μm thickness were fixed in cold acetone for 5 minutes at

room temperature. After blocking with PBS containing 2% BSA and 5% heat-inactivated normal goat serum, the sections were incubated with primary antibodies for 2 hours at 37°C. Primary antibodies used in this study are: rabbit anti-phospho-A-type lamin polyclonal antibodies at 1:50; mouse anti-human merosin (M-chain) monoclonal antibody (5H2) (Chemicon International, Temecula, CA) at 1:400; rabbit anti-lamin A polyclonal antibody (Sakaki et al., 2001) at 1:400; mouse anti-Pax7 monoclonal antibody (Developmental Studies Hybridoma Bank, Iowa City, IA) at 1:300. Sections were incubated with anti-rabbit IgG antibody conjugated with Alexa-Fluor-488 and anti-mouse IgG antibody conjugated with Alexa-Fluor-568 (Invitrogen, Carlsbad, CA) at 1:500 for 45 minutes at room temperature. To enhance the immunoreactions, we used Can Get Signal immunostain solution A (Toyobo, Osaka, Japan) to dilute primary and secondary antibodies. Sections were observed under a Zeiss Axiophot 2 microscope (Carl Zeiss, Oberkochen, Germany).

Immunoblot analysis

For biopsied muscle specimens, 20 slices of 10 μm cryosections were immediately sonicated in SDS sample buffer [50 mM Tris-HCl (pH 6.8), 2% SDS, 1% glycerol (v/v), 0.1% bromophenol blue, 6% 2-mercaptoethanol] and boiled for 5 minutes at 95°C. The lysates were centrifuged at 100,000 ***g*** at 4°C for 5 minutes. The supernatants were subjected to SDS-PAGE and the proteins were transferred to Immobilon-P membranes (Millipore). The membranes were blocked with blocking buffer [2% BSA in Tris-buffered saline (TBS) containing 0.05% Tween-20] at room temperature for 1 hour, then incubated with anti-Ser458-*P* antibody diluted in Can Get Signal solution 1 (Toyobo) at 1:1000 at 4°C overnight. The anti-Ser458-*P* antibody was followed with Histofine simple stain MAX-PO (Nichirei Biosciences, Tsukiji, Tokyo, Japan) diluted in Can Get Signal solution 2 at 1:500 at room temperature for 45 minutes. Recognized proteins were visualized by enhanced chemiluminescence plus detection reagent (GE Healthcare).

Plasmid construction and mutagenesis

To generate FLAG-tagged wild-type human lamin A, the N terminus of human lamin A was amplified by PCR using the following primers: 5′-GGAATTCA-CCATGGACTACAAAGACGATGACGACAAGGAGACCCCGTCCCAGCGG-3′ and 5′-CTCGCGGCTGACCACCTCTT-3′. PCR product was digested with *Eco*RI and *Acc*I, and subcloned into full-length human prelamin A in pUC19 (a kind gift from Howard J. Worman, Columbia University, NY). FLAG-tagged lamin A cDNA was cut out by digestion with *Eco*RI and *Xba*I, and subcloned into pcDNA3.1 (Invitrogen). Each of the mutant lamin A constructs was made by site-directed mutagenesis (Horton et al., 1989) using the primers listed in supplementary material Table S2. Arg453Trp and Arg471Cys mutants were made by combining primers LMNA1386 and R453W-Fw with R453W-Rv and LMNA2579, and LMNA1386 and R471C-Fw with R471C-Rv and LMNA2579, respectively.

Human full-length Akt1 was amplified by PCR using an Akt1 cDNA construct (a gift from Yukiko Gotoh, University of Tokyo, Japan) (Masuyama et al., 2001) and subcloned into pcDNA3 (Invitrogen). Then, a hemagglutinin (HA) tag was added at the C-terminal end, yielding wtAkt–HA. The constitutively active form of Akt (myrAkt–HA) was generated by adding a myristoylation site derived from murine Src tyrosine kinase to the N-terminal end of the Akt–HA described above (Andjelkovic et al., 1997; Manning and Cantley, 2007).

For the in vitro kinase assay, the C-terminal tail domain of lamin A (amino acids 411–553) was amplified by PCR using the following primers: 5′-CATATGG-GTGGGGGCAGCGTCACCAAAAAG-3′ and 5′-GGGATCCTTAGTCGTCCT-CAACCACAGTCACTGAGC-3′. PCR product was ligated with pGEM-T-easy (Promega, Madison, WI), digested with *Nde*I and *Bam*HI, and subcloned into pET 15b vector (Merck, Darmstadt, Germany).

The sequences of all constructs were verified by DNA sequencing.

Cell culture and transfection

African green-monkey kidney fibroblast cell line COS-7 cells and mouse myoblast cell line C2 cells were cultured in DMEM (Sigma, St Louis, MO) supplemented with 10% FBS (Invitrogen) at 37°C in a humidified atmosphere of 5% CO_2. Before transfection, the medium was replaced with serum-free DMEM. The cells were transiently transfected using FuGENE HD transfection reagent (Roche Diagnostics, Indianapolis, IN). After 8–12 hours transfection, DMEM supplemented with 20% FBS was added to the dishes to adjust the FBS concentration in the medium to 10%. The cells were used for each experiment 48 hours after transfection.

Immunoprecipitation and alkaline phosphatase treatment

COS-7 cells were transfected with 10 μg wild-type lamin A or Arg453Trp lamin A construct. The cells were lysed in 1.0 ml lysis buffer containing 50 mM Tris-HCl (pH 7.5), 150 mM NaCl, 1% Nonidet P-40, 0.5% sodium deoxycholate and Complete Protease Inhibitor Cocktail (Roche Diagnostics). The lysates were incubated at 4°C for 30 minutes with gentle rotation and then centrifuged at 15,000 ***g*** at 4°C for 30 minutes. The supernatants were collected and their protein concentrations were determined using a protein assay kit (Bio-Rad, Hercules, CA). For immunoprecipitation, the protein concentration of the cleared lysates was adjusted to 1.0 μg/μl and 40 μl anti-FLAG M2 affinity gel (Sigma) was added. The mixtures were incubated at 4°C overnight. The resulting immune complexes were washed three times with TBS and two times with alkaline phosphatase buffer (AP buffer) containing 50 mM Tris-HCl (pH 9.0) and 1 mM $MgCl_2$. The immune complexes were incubated with calf intestine alkaline phosphatase (Takara Bio, Shiga, Japan) in AP buffer at 37°C overnight. The proteins were eluted by boiling at 95°C for 5 minutes in SDS sample buffer. Immunoblot analysis was performed as described above. To detect FLAG-tagged lamin A, we used mouse anti-FLAG M2 monoclonal antibody (Sigma) diluted in PBS containing 5% skim milk at 1:2500.

Immunocytochemistry

Human skin fibroblasts from healthy individuals (control), AD-EDMD patients with a *LMNA* Leu102Pro or Arg453Trp mutation, and transfected C2 myoblasts were plated onto 12 mm cover glass coated with type I collagen. The cells were fixed in methanol for 10 minutes at −20°C. The steps were as described under Immunohistochemistry.

Akt kinase assay

In mammalian cell experiments, COS-7 cells or C2 myoblasts were co-transfected with 5 μg each of Akt–HA construct and FLAG–lamin A construct. The cells were lysed in 1.0 ml lysis buffer supplemented with 50 mM sodium fluoride, 1 mM sodium orthovanadate and 1 mM phenylmethylsulfonyl fluoride. FLAG–lamin A was immunoprecipitated as described above. The resulting immune complexes were washed two times with lysis buffer and two times with TBS. The proteins were eluted by boiling at 95°C for 5 minutes in SDS sample buffer. Immunoblot analysis was performed as described above. For the detection of phosphorylated proteins, Blocking One-P blocking solution (Nacalai Tesque, Kyoto, Japan) was used. Mouse anti-HA monoclonal antibody (16B12 clone; Covance, Princeton, NJ) was used at 1:1000, rabbit anti-phospho-Akt (Ser473) monoclonal antibody (Cell Signaling Technology, Danvers, MA) was used at 1:1000, and rabbit anti-actin polyclonal antibody (Nichirei) was used at 1:2000.

For the in vitro kinase assay, the C-terminal tail domain of lamin A (LA-T) was in-vitro translated as a His-tagged protein using the S30 T7 High-Yield Protein Expression System (Promega) according to the manufacturer's instructions. The LA-T was purified with Ni-NTA agarose and eluted with elution buffer containing 50 mM NaH_2PO_4, 300 mM NaCl, 250 mM imidazole, followed by dialysis against 20 mM MOPS-NaOH (pH 8.0), 1 mM EDTA, 5% glycerol, 50 mM NaCl at 4°C overnight. Approximately 0.5 μg His-tagged protein was incubated with 5 ng recombinant active Akt1 (Millipore) in a reaction buffer consisting of 8 mM MOPS-NaOH (pH 7.0), 0.2 mM EDTA, 10 mM magnesium acetate, 100 mM ATP at 30°C for 30 minutes. The reaction was terminated by the addition of SDS sample buffer. Immunoblot analysis was performed as described above. For the detection of His-tagged proteins, mouse anti-His-tag monoclonal antibody (Merck) was used at 1:2000.

We thank May Malicdan (National Center of Neurology and Psychiatry) for reviewing the manuscript, and Kamako Goto, Mieko Ohnishi, Yuriko Kure and Megumo Ogawa (National Center of Neurology and Psychiatry) for technical assistance. This study was supported by a Research on Psychiatric and Neurological Diseases and Mental Health of Health Labour Sciences Research Grant; by a Research Grant (20B-12, 20B-13) for Nervous and Mental Disorders from the Ministry of Health, Labor and Welfare of Japan; by a grant from the Japan Foundation for Neuroscience and Mental Health; by grants from the Human Frontier Science Program; by a KAKENHI grant (21591104) from the Japan Society for the Promotion of Science; by Research on Publicly Essential Drugs and Medical Devices from the Japanese Health Sciences Foundation; and by the Program for Promotion of Fundamental Studies in Health Sciences of the National Institute of Biomedical Innovation (NIBIO).

Supplementary material available online at
http://jcs.biologists.org/cgi/content/full/123/22/3893/DC1

References

Andjelkovic, M., Alessi, D. R., Meier, R., Fernandez, A., Lamb, N. J., Frech, M., Cron, P., Cohen, P., Lucocq, J. M. and Hemmings, B. A. (1997). Role of translocation in the activation and function of protein kinase B. *J. Biol. Chem.* **272**, 31515-31524.

Bonne, G., Di Barletta, M. R., Varnous, S., Becane, H. M., Hammouda, E. H., Merlini, L., Muntoni, F., Greenberg, C. R., Gary, F., Urtizberea, J. A. et al. (1999). Mutations in the gene encoding lamin A/C cause autosomal dominant Emery-Dreifuss muscular dystrophy. *Nat. Genet.* **21**, 285-288.

Bonne, G., Yaou, R. B., Beroud, C., Boriani, G., Brown, S., de Visser, M., Duboc, D., Ellis, J., Hausmanowa-Petrusewicz, I., Lattanzi, G. et al. (2003). 108th ENMC International Workshop, 3rd Workshop of the MYO-CLUSTER project: EUROMEN, 7th International Emery-Dreifuss Muscular Dystrophy (EDMD) Workshop, 13-15 September 2002, Naarden, The Netherlands. *Neuromuscul. Disord.* **13**, 508-515.

Boriani, G., Gallina, M., Merlini, L., Bonne, G., Toniolo, D., Amati, S., Biffi, M., Martignani, C., Frabetti, L., Bonvicini, M. et al. (2003). Clinical relevance of atrial